

Quantifying optimal resource allocation strategies for controlling epidemics

Biplab Maity^a, Swarnendu Banerjee^{a,c,1,*}, Abhishek Senapati^{a,b,1,*}, Joydev Chattopadhyay^a

^a*Agricultural and Ecological Research Unit, Indian Statistical Institute, 203, B. T. Road, Kolkata 700108, India*

^b*Center for Advanced Systems Understanding (CASUS), Goerlitz, Germany*

^c*Copernicus Institute of Sustainable Development, Utrecht University, PO Box 80115, 3508 TC, Utrecht, The Netherlands*

Abstract

Frequent emergence of communicable diseases has been a major concern worldwide. Lack of sufficient resources to mitigate the disease-burden makes the situation even more challenging for lower-income countries. Hence, strategy development towards disease eradication and optimal management of the social and economic burden has garnered a lot of attention in recent years. In this context, we quantify the optimal fraction of resources that can be allocated to two major intervention measures, namely reduction of disease transmission and improvement of healthcare infrastructure. Our results demonstrate that the effectiveness of each of the interventions has a significant impact on the optimal resource allocation in both long-term disease dynamics and outbreak scenarios. Often allocating resources to both strategies is optimal. For long-term dynamics, a non-monotonic behavior of optimal resource allocation with intervention effectiveness is observed which is different from the more intuitive strategy recommended in case of outbreaks. Further, our result indicates that the relationship between investment into interventions and the corresponding outcomes has a decisive role in determining optimal strategies. Intervention programs with decreasing returns promote the necessity for resource sharing. Our study provides a fundamen-

*Corresponding author

Email: abhishekiz4u04@gmail.com; swarnendubanerjee92@gmail.com

¹Equal contribution

tal insight into determining the best response strategy in case of controlling epidemics under resource-constrained situations.

Keywords: Resource allocation, Disease outbreak, Intervention strategy, Production function

1. Introduction

Infectious diseases like Influenza, Severe Acute Respiratory Syndrome (SARS), Ebola, and most recently COVID-19 spread throughout a population within a short time making it a cause of utmost concern for human society (Fraser et al., 2009; Colizza et al., 2007; Hufnagel et al., 2004; Legrand et al., 2007; Zhang et al., 2020a; Mahase, 2020; Gubler, 2002). Lack of appropriate health policies, protective medical equipment such as disposable gloves, surgical masks and so on, poorly developed infrastructure, and shortage of medical personnel make it even more challenging for low-income countries to mitigate the health crisis during an ongoing outbreak (Oshitani et al., 2008; Hopman et al., 2020). This can be well understood, for instance, by considering the severe impact of Ebola on West African countries like Nigeria, Liberia, and Sierra Leone where there was an estimated shortage of 7.2 million doctors and health workers (Gostin, 2014; Gostin and Friedman, 2015). Furthermore, estimates also indicate that nearly 79% of total available hospital beds would be required for patients due to Influenza in the lower income countries with an incidence rate of 35%. This estimate becomes more than 100% in countries like Bangladesh and Nepal even at the incidence rate of 15% (Oshitani et al., 2008). Therefore, the allocation of resources in an optimal way becomes a necessary component of public health response toward controlling the spread of infectious diseases.

A simplistic way to look at control of infectious disease outbreaks is either by prevention of transmission through non-pharmaceutical interventions (NPI) such as social distancing, personal hygiene, contact tracing, and early detection or improvement of recovery rate by providing better medical treatment. World Health Organization (WHO, 2005, 2020) and governmental health agencies in many countries publish disease prevention protocols to fight against disease outbreaks (Benson et al., 2009; Siegel et al., 2007; Adhikari et al., 2020). There are also campaigns, often using various social networking websites and educational programs to increase awareness among people about a particular disease. In absence of a proper effective vaccine

or vaccination strategy, the implementation of various preventive measures helps to diminish the contact among the infected and susceptible individuals thereby reducing the transmission rate. Although NPIs are likely to be effective at early stages but often it is not possible to keep the disease transmission under control, especially, when there is a sudden flare-up of cases. Additionally, there are also difficulties in implementing control measures like lockdown or travel restrictions due to huge economic and societal costs, mainly in developing countries (Angulo et al., 2021; Ngonghala et al., 2020). In such a case, it is important to ramp up hospital infrastructure and consequently prioritize the quality of treatment which would influence the recovery of infected individuals thus reducing the potential impact of an epidemic (Farmer, 2001; Mosadeghrad, 2014; Emanuel et al., 2020). Such measures would include increasing the number of hospital beds (Sacchetto et al., 2020), setting up temporary medical units, training program of health-care personnel (Oshitani et al., 2008), and procuring more medical equipment and medicines.

Designing efficient and feasible control strategies that maintain a balance between the implementation of pharmaceutical as well as non-pharmaceutical interventions in a resource-constrained situation is essential to reduce the potential impact of disease burden. However, in both cases, effectiveness of the interventions plays a key role in determining the success of the implemented strategies. One intervention measure is said to be more effective than the other, if a better recovery rate or a reduced transmission rate is achieved at the expense of the same resource. For instance, in order to mitigate Ebola and SARS, symptom monitoring program becomes a more effective measure than quarantine, whereas the benefit of quarantine over symptom monitoring has been observed for diseases like Influenza and smallpox (Peak et al., 2017). Also, face covering appears to be a more effective way to prevent COVID-19 than that of quarantine and maintaining social distancing measures (Zhang et al., 2020b). On the other hand, treatment protocol using drugs like Remdesivir was shown to be more effective than that of Hydroxychloroquine during the early stages of the COVID-19 pandemic (Beigel et al., 2020; Group, 2020). Furthermore, the relationship between invested resources and the corresponding outcome from an intervention program, also known as the production function, plays a decisive role in determining optimal strategies (Brandeau et al., 2005). Since the outcome of an intervention depends on its effectiveness, the later influences the steepness of a particular type of production function. Hence, it becomes important to design resource

allocation policies by taking into account the effectiveness of available intervention programs and their corresponding production functions to evaluate their performance in disease mitigation.

To analyse a range of possible scenarios under specific epidemic situations, mathematical models have been used as an important and reliable tool to guide policy making and implementing different intervention programs. In this regard, several attempts have been made that investigated different aspects of optimal resource allocation strategies (Medlock and Galvani, 2009; Alistar et al., 2014; Brandeau and Zaric, 2009; Hansen and Day, 2011; Worby and Chang, 2020; Brandeau et al., 2003; Senapati et al., 2019; Calabrese and Demers, 2022; Ghosh et al., 2021; Bolzoni et al., 2019). Many of these studies have focused on resource allocation to only prevention programs related to vaccination (Medlock and Galvani, 2009), or transmission reductions like face mask distribution (Worby and Chang, 2020) and testing (Calabrese and Demers, 2022; Ghosh et al., 2021). Few studies have also considered resource allocation between two different strategies such as vaccination and isolation but did not take into account any explicit trade-off between them (Hansen and Day, 2011; Bolzoni et al., 2019). Thus these studies lack in providing a theoretical framework to study optimal resource allocation between two main classes of intervention strategies - transmission reduction and improving healthcare infrastructure where there can be trade-offs between the two. While a recent study examined the allocation of resources between prevention and treatment, the role of effectiveness of the former was not explored (Alistar et al., 2014). Moreover, the study was based on HIV transmission and hence did not consider a recovered class which might be relevant for other diseases. For the same reason, the optimal strategy was determined considering only specific types of production functions.

In this study, we fill this gap and attempt to provide a general understanding of how limited resources may be allocated between transmission-reducing and recovery-improvement programs taking into account the effectiveness of both the types of interventions. Using a simple SIR model, we quantify the optimal fraction of resources required to minimize the impact of disease burden under both long-term disease dynamics and outbreaks. We study the role of different types of production functions and explored how the optimal strategy varies with the effectiveness of the intervention measures. Furthermore, since there is a delay in reporting new infections and proper knowledge about the disease is not available at early stages, we also quantify the optimal fraction of resources in the presence of delay in implementing interventions.

2. Methods

2.1. Model

We consider the well-known compartmental Susceptible-Infected-Recovered (SIR) model ([Anderson and May, 1992](#); [Breda et al., 2012](#)) to represent the disease dynamics. At time t , the fractions of susceptible, infected, and recovered population are denoted by $S(t)$, $I(t)$, and $R(t)$ respectively which satisfies the constraint $S(t) + I(t) + R(t) = 1$. The rate of change of the fraction of people in each compartment can be described as follows:

$$\begin{aligned}\frac{dS}{dt} &= \mu - \beta_0 SI - \mu S, \\ \frac{dI}{dt} &= \beta_0 SI - \gamma_0 I - \mu I, \\ \frac{dR}{dt} &= \gamma_0 I - \mu R.\end{aligned}\tag{1}$$

Here, β_0 is the disease transmission rate, μ is the birth and death rate, and γ_0 is the recovery rate. The basic reproduction number, \mathcal{R}_0 , defined as the average number of secondary cases appearing from an average primary case in an entirely susceptible population, can be obtained as $\mathcal{R}_0 = \frac{\beta_0}{\gamma_0 + \mu}$.

We introduce control strategies utilizing available resources among competing prevention and treatment programs. Here, one can think of the available resources as the total financial budget for government investment in healthcare. A natural consequence of the allocation of resources is an alteration in disease transmission rates and recovery rates that affect epidemic outcomes. Here, a fraction u of total available resources is allocated for implementing transmission-reducing strategies, and the remaining fraction, i.e., $(1 - u)$ is devoted to improving healthcare infrastructure (see the schematic in [Fig. 1](#)). The fact that the total available resources to reduce disease burden are fixed, signifies a trade-off between allocations to the two types of competing intervention programs.

The relationship between the invested resources and outcomes of intervention programs, described by the production function, determines the true impact of public health interventions. We denote $F_{\beta_0}(u)$ and $F_{\gamma_0}(1 - u)$ as

the production functions associated with transmission-reducing and recovery-improvement programs, respectively. To reflect the effect of resource implementation, we replace β_0 and γ_0 in model (1) by $F_{\beta_0}(u)$ and $F_{\gamma_0}(1 - u)$ respectively (see the schematic in Fig. 1). So the model with interventions can be written as

$$\begin{aligned}\frac{dS}{dt} &= \mu - F_{\beta_0}(u)SI - \mu S, \\ \frac{dI}{dt} &= F_{\beta_0}(u)SI - F_{\gamma_0}(1 - u)I - \mu I, \\ \frac{dR}{dt} &= F_{\gamma_0}(1 - u)I - \mu R.\end{aligned}\tag{2}$$

Now, production functions, F_{β_0} and F_{γ_0} , can be broadly categorized into three types as described below. For each incremental investment in the intervention programs, the associated production function, F_{β_0} (F_{γ_0}) gives decreasing, constant, or increasing returns to scale if the corresponding reduction (improvement) in the transmission (recovery) rate is increasingly smaller, remains constant or increasingly larger respectively (see Fig. 2) (Brandeau et al., 2003; Brandeau and Zaric, 2009).

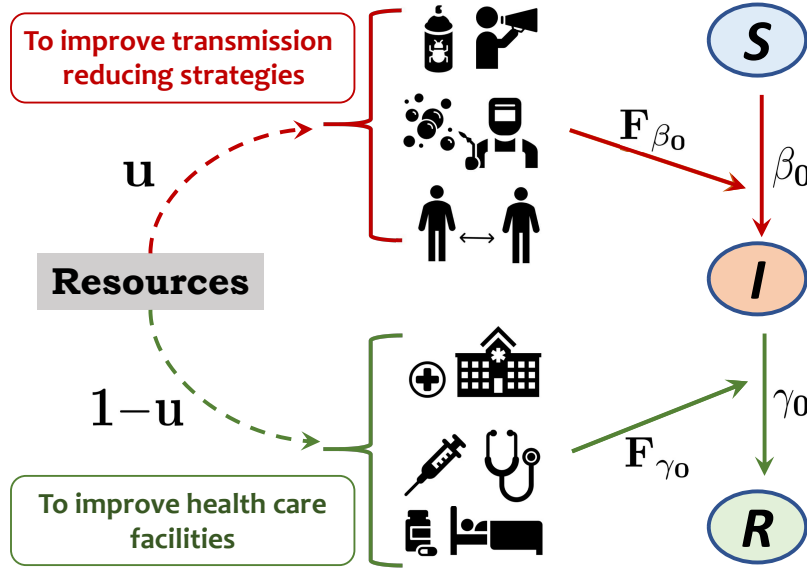


Figure 1: Optimal resource allocation. The total resources available for disease control are allocated to two broad classes of interventions namely transmission-reducing interventions like awareness programs, personal hygiene, social distancing, etc., and the intervention programs that would improve health care facilities which in turn shortens the infectious period and speed up the process of recovery. Here, u is the fraction of the total available resources allocated to the transmission-reducing interventions and the remaining $(1 - u)$ fraction is allocated to improve healthcare facilities. This process of resources allocation is incorporated in the classical SIR model by introducing the production functions, F_{β_0} and F_{γ_0} , that will reflect the effect of resource allocation in transmission rate (β_0) and recovery rate (γ_0) respectively.

For the sake of comparison, we assume that three types of returns considered for F_{β_0} (F_{γ_0}) are equivalent to each other at the two extreme cases, i.e., when $u = 0$ or $u = 1$ (see Fig. 2). Further, it is important to note that there is always a limited realizable benefit from an intervention program regardless of investment (Brandeau et al., 2005, 2003). This implies that there always will be a lower limit to the reducible transmission rate and an upper limit to the achievable recovery rate. However, these limits are dependent on the effectiveness of the intervention strategies. For the same resources, a more effective intervention measure implies more reduction (increase) in transmission (recovery) rate (see Fig. 2).

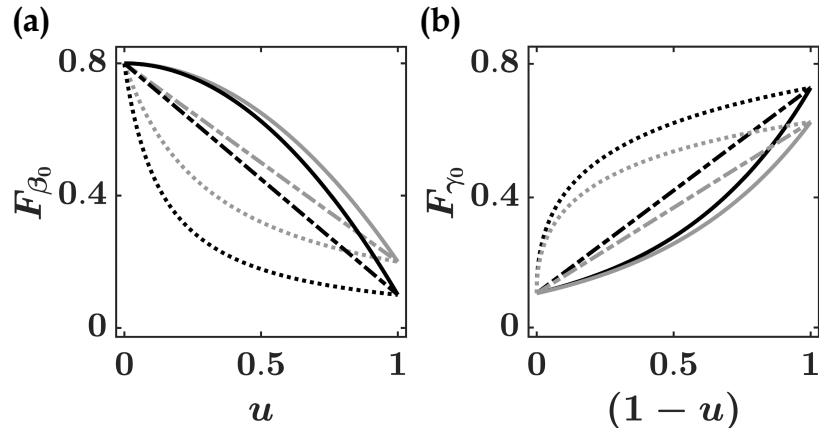


Figure 2: Different types of production functions: (a) $F_{\beta_0}(u)$ and (b) $F_{\gamma_0}(1-u)$ corresponding to transmission-reducing and recovery-improvement interventions respectively. Here solid, dashed, and dotted lines represent increasing, constant and decreasing returns to scale respectively. In each of (a) and (b), the production functions with lower and higher effectiveness parameters are presented in grey and black colour respectively. For specific forms of F_{β_0} and F_{γ_0} , refer to [Appendix B](#), [Fig. B.10](#) caption.

We consider the production functions, $F_{\beta_0}(u) = \frac{\beta_0}{1 + \beta_e u}$, and $F_{\gamma_0}(1-u) = \gamma_0(1 + \gamma_e(1-u))$, where the parameter β_e indicates the effectiveness of transmission-reducing interventions, and the parameter γ_e denotes the effectiveness of recovery-improving interventions. Here, F_{β_0} and F_{γ_0} have decreasing and constant returns to scale, respectively. The motivation for such consideration comes from several theoretical as well as empirical studies on resource allocation for HIV prevention programs like needle exchange ([Kaplan, 1995](#)) and condom distribution ([Zaric and Brandeau, 2001](#); [Alistar et al., 2014](#)) and treatment programs like antiretroviral therapy ([Lima et al., 2008](#); [Alistar et al., 2014](#)) and methadone maintenance ([Zaric et al., 2000a,b](#)). However, our consideration of the effectiveness of recovery-improving interventions is different from that of the treatment effectiveness in ([Alistar et al., 2014](#)) as the later does not increase the recovery rate but reduces the infectivity of susceptibles after treatment. It is to be noted that if both β_e and γ_e are set to zero, the model (2) will be reduced to the original model (1). Now in the presence of control strategy, we define control reproduction number

\mathcal{R}_0^c as

$$\begin{aligned}\mathcal{R}_0^c &= \frac{F_{\beta_0}(u)}{F_{\gamma_0}(1-u) + \mu} \\ &= \frac{\beta_0}{(1 + \beta_e u)(\gamma_0(1 + \gamma_e(1-u)) + \mu)}.\end{aligned}$$

We use the phrases *improving health care facilities* and *improving recovery*, and also *transmission-reducing* and *prevention* programs interchangeably throughout the paper.

2.2. Model parametrization and simulations

We take the numerical value of the model parameters like birth/death rate, disease transmission rate, and recovery rate from previous studies. The parameters related to effectiveness are varied in our study. The initial conditions, S_0 and I_0 are chosen with the assumption that initially, almost everyone in the population is susceptible. All simulations in the paper are done using parameters in Table 1 unless specified otherwise.

To obtain the optimal fraction of resources numerically, first, the values of u are spaced linearly between 0 to 1 with suitable step-length and for each value of u , we integrate the model (2) numerically using *ode45* in MATLAB (Mathworks, R2018a) and calculate the objective function. We select that value of u as optimal for which the objective function gives the minimum value.

3. Results

We investigate the problem of optimal resource allocation in two scenarios: (i) long-term or endemic dynamics of the disease, and (ii) dynamics of the disease during an outbreak. In the first scenario, the demographic factors are considered, i.e., the birth and death rates are non-zero and in the second scenario, we ignore birth and natural death rates to capture the short-term dynamics of the disease.

In the following subsections, we first describe the results for both of the long-term and outbreak scenarios for our model. Subsequently, we also analyze the model considering all three types of returns to scale for each of F_{β_0} and F_{γ_0} and all their possible combinations.

Parameters	Description	Value	References
μ	Natural birth and death rate of human	$\frac{1}{70}$ year ⁻¹	(Keeling and Rohani, 2011; Martcheva, 2015)
β_0	Transmission rate	0.8 day ⁻¹	(Keeling and Rohani, 2011)
γ_0	Recovery rate	0.1 day ⁻¹	(Keeling and Rohani, 2011; Deka and Bhattacharyya, 2019)
β_e	Effectiveness of transmission-reducing interventions	Varied	-
γ_e	Effectiveness of recovery-improving interventions	Varied	-
S_0, I_0	Initial proportion of susceptible, infected individuals	0.999, 0.001	Assumed

Table 1: Description of parameters for the model (1).

3.1. Resource allocation for long-term dynamics of the disease

To control long-term disease persistence, we take the proportion of infected individuals at equilibrium (I^*) as the objective function which is to be minimized in the presence of allocated resources. From the resource implemented model (2), we can find the proportion of susceptible (S^*) and infected (I^*) individuals at equilibrium analytically using null-isoclines as

$$\begin{aligned}
 S^* &= \begin{cases} 1/\mathcal{R}_0^c & \text{if } \mathcal{R}_0^c > 1 \\ 1 & \text{if } \mathcal{R}_0^c \leq 1 \end{cases} \\
 I^* &= \begin{cases} \frac{\mu}{F\beta_0}(\mathcal{R}_0^c - 1) & \text{if } \mathcal{R}_0^c > 1 \\ 0 & \text{if } \mathcal{R}_0^c \leq 1 \end{cases} \quad (3)
 \end{aligned}$$

When $\mathcal{R}_0^c > 1$, the endemic equilibrium is locally asymptotically stable while the disease-free equilibrium exists but is unstable. The equilibria merge when $\mathcal{R}_0^c = 1$, and only a stable disease-free equilibrium exists when $\mathcal{R}_0^c < 1$. This implies that the number of infected individuals asymptotically approaches a non-zero endemic level when $\mathcal{R}_0^c > 1$ and zero when $\mathcal{R}_0^c \leq 1$.

To find the optimal fraction of resources in the former case, i.e, when $\mathcal{R}_0^c > 1$, we differentiate I^* with respect to u and set it equal to zero. Then simple algebraic manipulation allows us to solve for u , which we denote as u_1 :

$$u_1 = \frac{\beta_e(\gamma_0 + \gamma_0\gamma_e + \mu) - \sqrt{\beta_0\beta_e\gamma_0\gamma_e}}{\beta_e\gamma_0\gamma_e}. \quad (4)$$

It is important to note that the fraction of resources allocated must be constrained between 0 and 1. Taking this into account, it can be shown that when $\mathcal{R}_0^c \leq 1$, the optimal fraction of resources can lie anywhere in a certain interval $[u_{l_1}, u_{l_2}] \subseteq [0, 1]$ (see [Appendix A](#)). Hence, one can define the optimal fraction of resources to prevent transmission in case of long-term disease dynamics, u_{long}^* , as follows:

$$u_{\text{long}}^* = \left\{ \begin{array}{ll} 0 & \text{if } u_1 \leq 0 \\ u_1 & \text{if } 0 < u_1 < 1 \\ 1 & \text{if } u_1 \geq 1 \\ [u_{l_1}, u_{l_2}] & \subseteq [0, 1] \end{array} \right\} \begin{array}{l} \mathcal{R}_0^c > 1 \\ \mathcal{R}_0^c \leq 1 \end{array} \quad (5)$$

Now, we explore the behavior of u_{long}^* with respect to the effectiveness of intervention programs β_e, γ_e when $\mathcal{R}_0^c > 1$. Here, $\lim_{\beta_e \rightarrow 0} u_{\text{long}}^* = 0$ (as $\lim_{\beta_e \rightarrow 0} u_1 \rightarrow -\infty$) indicates that when β_e is too low the optimal strategy is to allocate the entire resources to recovery improvement programs. This holds true until a threshold, $\beta_e^l = \frac{\beta_0\gamma_0\gamma_e}{(\gamma_0 + \gamma_0\gamma_e + \mu)^2}$ above which u_{long}^* increases with β_e implying the need to allocate increasing fractions of resources to prevention programs (see [Fig. 3\(a\)](#)). It is interesting to note that β_e^l is non-monotonic in γ_e . As a result, we can see that the threshold for $\gamma_e = 1$ shifts towards right from the threshold for $\gamma_e = 0.5$, but for higher values of γ_e ($\gamma_e=2, 5$), the threshold shifts toward left (see [Fig. 3\(a\)](#)).

Similarly, $\lim_{\gamma_e \rightarrow 0} u_{\text{long}}^* = 1$ (as $\lim_{\gamma_e \rightarrow 0} u_1 \rightarrow +\infty$) implies that when γ_e is too low, the optimal strategy is to devote entire resources to transmission-reducing programs. Again, this holds true only until a threshold $\gamma_e^l = \frac{\beta_e(\gamma_0 + \mu)^2}{\beta_0\gamma_0}$ above which u_{long}^* starts to decrease with γ_e . This trend persists until a second threshold, $\tilde{\gamma}_e = \frac{4\beta_e(\gamma_0 + \mu)^2}{\beta_0\gamma_0}$ after which the optimal strategy is to allocate decreasing fractions of resources toward treatment programs (see [Fig. 3\(b\)](#)). Furthermore, the sensitivity of our findings to the baseline model parameters (β_0, γ_0 , and μ) is discussed in [Appendix A](#) and displayed in [Fig. A.8](#).

In order to better understand the role of the effectiveness parameters in optimal resource allocation, the two-parameter space $(\beta_e - \gamma_e)$ can be divided into four regions (see Fig. 3(c)). We vary β_e and γ_e till the values such that only one type of intervention alone cannot achieve an asymptotically stable disease-free state. Here [1], [2], and [3] are associated with the locally asymptotically stable endemic state of the prevalence (where $\mathcal{R}_0^c > 1$). In [1] and [3], the optimal strategy is to allocate entire resources to recovery improvement (i.e., $u_{\text{long}}^* = 0$) and transmission-reducing programs (i.e., $u_{\text{long}}^* = 1$) respectively. In [2], there will be unique optimal strategies between 0 and 1 determined by the effectiveness parameters which signifies the need to allocate resources to both prevention and treatment. The resulting control reproduction number can then be expressed as:

$$\mathcal{R}_0^{\text{long}} = \frac{\sqrt{\beta_0 \beta_e \gamma_0 \gamma_e}}{\beta_e(\gamma_0 + \mu) + \gamma_0 \gamma_e(1 + \beta_e) - \sqrt{\beta_0 \beta_e \gamma_0 \gamma_e}}. \quad (6)$$

Here, the lines separating [2] from [1] and [3] is formed by the threshold values β_e^l and γ_e^l mentioned above. [4] corresponds to $\mathcal{R}_0^c \leq 1$ where u_{long}^* is not unique but can vary between certain ranges (see expression (A.2) and Fig. A.9 in Appendix A). With increasing β_e and γ_e , the range of values of u_{long}^* in [4] increases, signifying a greater flexibility of choice of optimal strategy (see Fig. A.9, Appendix A). The line $\mathcal{R}_0^c = 1$ denotes the borderline between [4] and [2] (red line in Fig. 3(c)). It can also be interpreted as the line of critical thresholds $\beta_e^{\text{crit}}(\gamma_e)$ or $\gamma_e^{\text{crit}}(\beta_e)$, i.e., the least values of β_e and γ_e which will lead to stable disease-free state asymptotically under optimal resource allocation. Overall, we see that the optimal strategy changes from allocating resources in a single intervention in [1] and [3] to dividing resources between both interventions in [2] and [4] under different effectiveness parameters.

Now we quantify the relative impact of resource allocation on disease dynamics. For this, we consider the uncontrolled epidemic (i.e., when both β_e and γ_e are zero) as the baseline scenario. We then calculate the percentage of relative reduction (RR_{I^*}) of the objective functions I^* by varying the effectiveness parameters in presence of optimal resources (see Fig. 3(d)). For small values of γ_e , such as $\gamma_e = 0.5, 1, 2$, if we vary β_e in the interval $0 \leq \beta_e \lesssim 2$, the relative reduction in I^* by allocating the available resources optimally stays almost same with approximately 38%, 57%, 76% respectively (see Fig. 3(d)). Since, for these γ_e values within $0 \leq \beta_e \lesssim 2$, $u_{\text{long}}^* = 0$ is

found to be optimal (see Fig. 3(a)), therefore we do not observe any role of β_e on the reduction of I^* . However, if we increase β_e further ($2 \leq \beta_e \leq 6$), we see gradual increase in RR_{I^*} (see Fig. 3(d)). This is because u_{long}^* is non-zero in this case and both β_e, γ_e have certain contributions. If γ_e is fixed to a relatively higher value, such as $\gamma_e = 5$, RR_{I^*} can reach about 95% (see Fig. 3(d)).

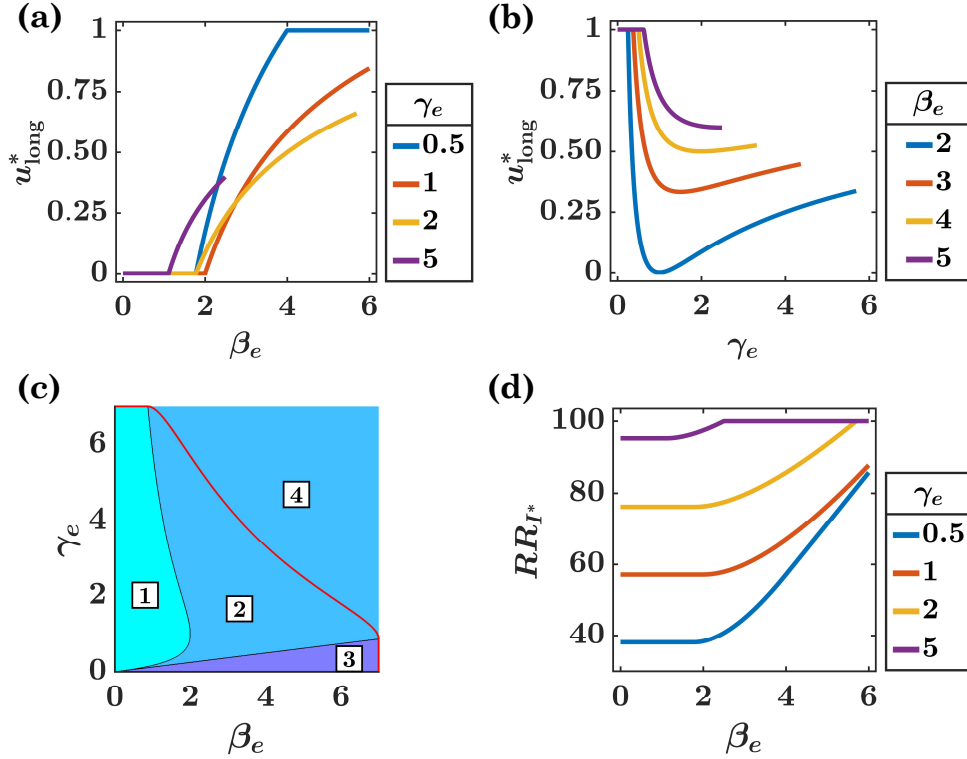


Figure 3: Role of effectiveness parameters in determining the optimal fraction of allocated resources to control disease dynamics in long-term scenario. Optimal fraction of resources (a) with respect to β_e , (b) with respect to γ_e , (c) when both the effectiveness parameters, β_e and γ_e , are varied simultaneously. The red line in (c) represents $\mathcal{R}_0^c = 1$. Here, unique u_{long}^* is associated with $\mathcal{R}_0^c > 1$ (displayed as **1**, **2** and **3**), while non-unique u_{long}^* is associated with $\mathcal{R}_0^c \leq 1$ (displayed as **4**). **1** represents the region where $u_{\text{long}}^* = 0$, i.e., allocating entire resources toward the recovery-improvement programs is the optimal strategy. **3** represents the region where the allocation of entire resources towards transmission-reducing programs is the optimal strategy (i.e., $u_{\text{long}}^* = 1$). **2** and **4** represent the regions for resource sharing between two types of intervention programs. u_{long}^* has a unique value between 0 and 1 in **2**; u_{long}^* lies within an interval in **4**. (d) Relative reduction of I^* with respect to β_e for different values of γ_e .

3.2. Resource allocation for an outbreak scenario

For an outbreak scenario, we ignore natural birth and death in our model, i.e., we fix $\mu = 0$ in our model (2). In this case, the control reproduction

number can be expressed as $\mathcal{R}_0^{\text{out}} = \frac{\beta_0}{\gamma_0(1 + \beta_e u)(1 + \gamma_e(1 - u))}$. One can infer about the basic characteristics of an outbreak from the sign of $\frac{dI}{dt}|_{t=0}$ or equivalently $1 - S_0\mathcal{R}_0^{\text{out}}$. When $S_0\mathcal{R}_0^{\text{out}} > 1$, the number of infected individuals initially increases until it reaches its maximum and subsequently decays. When $S_0\mathcal{R}_0^{\text{out}} = 1$, the outbreak is initially in a stationary state and subsequently decays, and for $S_0\mathcal{R}_0^{\text{out}} < 1$, the outbreak is initially in a decaying state and remains to decay for all subsequent time. The maximum number of infected individuals at any one time, attained during the outbreak is defined as the peak of the epidemic. Since the peak is a primary indicator of the severity of an outbreak, lowering it is one of the primary goals for reducing the burden of outbreaks.

For this purpose, we derive the epidemic peak (I_{max}) analytically which can be expressed as follows (see [Appendix B](#))

$$I_{\text{max}} = \begin{cases} S_0 + I_0 - \frac{\left(\ln\left(S_0\mathcal{R}_0^{\text{out}}\right) + 1\right)}{\mathcal{R}_0^{\text{out}}} & \text{if } S_0\mathcal{R}_0^{\text{out}} > 1 \\ I_0 & \text{if } S_0\mathcal{R}_0^{\text{out}} \leq 1 \end{cases} \quad (7)$$

In case of initial growth of outbreak size (i.e., $S_0\mathcal{R}_0^{\text{out}} > 1$), the optimal fraction of resources can be obtained by differentiating I_{max} with respect to u , setting it equal to zero and solving algebraically (see [Appendix B](#)):

$$u_p = \frac{1}{2} \left(1 - \frac{1}{\beta_e} + \frac{1}{\gamma_e} \right) \quad (8)$$

Further, when the outbreak is initially in a stationary or decaying state, one can solve the inequality $S_0\mathcal{R}_0^{\text{out}} \leq 1$ for u to obtain the optimal fraction of resources in the form of an interval, $[u_{p_1}, u_{p_2}]$ (see [Appendix B](#)). As the fraction of allocated resources must be constrained between 0 and 1, a new quantity u_{peak}^* is defined as the optimal fraction of resources invested in transmission-reducing programs such that (see [Appendix B](#) for details)

$$u_{\text{peak}}^* = \begin{cases} \left. \begin{array}{l} 0 & \text{if } u_p \leq 0 \\ u_p & \text{if } 0 < u_p < 1 \\ 1 & \text{if } u_p \geq 1 \end{array} \right\} S_0\mathcal{R}_0^{\text{out}} > 1 \\ \left. \begin{array}{l} [u_{p_1}, u_{p_2}] \\ \subseteq [0, 1] \end{array} \right\} S_0\mathcal{R}_0^{\text{out}} \leq 1 \end{cases} \quad (9)$$

It can be observed from the Eq. (8) of u_p that u_{peak}^* depends only on the effectiveness of intervention programs β_e, γ_e when $S_0\mathcal{R}_0^{\text{out}} > 1$ and is independent of the transmission rate and recovery rate β_0, γ_0 . Similar to the long-term scenario, we explore the behavior of u_{peak}^* with respect to β_e and γ_e . Here, $\lim_{\beta_e \rightarrow 0} u_{\text{peak}}^* = 0$ (as $\lim_{\beta_e \rightarrow 0} u_p \rightarrow -\infty$) indicates that when β_e is too low, the optimal strategy is to allocate entire resources to recovery improvement programs. This holds true until a certain threshold, $\beta_e^p = \frac{\gamma_e}{1 + \gamma_e}$ after which u_{peak}^* increases with β_e . (Fig. 4(a)). Likewise, $\lim_{\gamma_e \rightarrow 0} u_{\text{peak}}^* = 1$ (as $\lim_{\gamma_e \rightarrow 0} u_p \rightarrow +\infty$) implies when γ_e is too low, the optimal strategy is to devote entire resources to transmission-reducing programs. Again, this holds true only until a threshold $\gamma_e^p = \frac{\beta_e}{1 + \beta_e}$ above which u_{peak}^* starts to decrease with γ_e (see Fig. 4(b)). Notably, in this case, the monotonic behaviour of u_{peak}^* with respect to β_e and γ_e indicates that the optimal control strategy is to allocate more resources towards intervention programs with better effectiveness (Fig. 4((a)(b))).

Parameter space $(\beta_e - \gamma_e)$ can be divided into four regions on the basis of optimal strategy (see Fig. 4(c)). Similar to Fig. 3(c), β_e and γ_e are varied till the values such that resource allocation to only one type of intervention cannot satisfy the condition for the initial decay state of the outbreak. [1], [2] and [3] correspond to $S_0\mathcal{R}_0^{\text{out}} > 1$, where the optimal fraction of resources towards transmission prevention, u_{peak}^* is given by 0, u_p and 1 respectively. In [2], where u_p is the unique optimal strategy, the control reproduction number for the outbreak scenario is given by:

$$\mathcal{R}_0^{\text{peak}} = \frac{4\beta_0\beta_e\gamma_e}{\gamma_0(\beta_e\gamma_e + \beta_e + \gamma_e)^2}. \quad (10)$$

The curves that separate [1] and [3] from [2] correspond to the threshold values β_e^p and γ_e^p respectively. In contrary to Fig. 3(c), here, [1] and [3] are symmetric about the line $\beta_e = \gamma_e$. This can be easily explained by the fact that both $\beta_e^p(\gamma_e)$ and $\gamma_e^p(\beta_e)$ satisfy the same underlying function. Further, it is interesting to note that $u_p(\beta_e, \gamma_e) = 1 - u_p(\gamma_e, \beta_e)$. This implies, if the effectiveness of prevention and treatment programs are reversed in case of certain diseases, then the optimal strategy is corresponding reversal of resource allocation. On optimal utilization of resources with increased effectiveness parameters, the outbreak is unable to initially grow ($S_0\mathcal{R}_0^{\text{out}} \leq$

1), which is represented by [4] (see Appendix B). Within [4], u_{peak}^* is non-unique and varies between certain ranges (see expression (B.4) in Appendix B). The line $S_0 \mathcal{R}_0^{\text{out}} = 1$ (red line) separates [4] from [2] in Fig. 4(c). It can also be interpreted as the line of critical values $\beta_e^{\text{crit}}(\gamma_e)$ or $\gamma_e^{\text{crit}}(\beta_e)$, i.e., least values of β_e and γ_e which are sufficient to prevent the outbreak from growing initially under optimal resource allocation.

With respect to the baseline scenario of uncontrolled epidemics ($\beta_e, \gamma_e = 0$), we calculate the percentage of relative reduction ($RR_{I_{\text{max}}}$) of I_{max} by varying the effectiveness parameters in presence of optimal resources (see Fig. 4(d)). For lower values of β_e , when $u_{\text{peak}}^* = 0$ is optimal (see Fig. 4(a)), we see from Fig. 4(d) that approximately 18%, 34%, 57% and 93% reduction can be achieved for $\gamma_e = 0.5, 1, 2$ and 5 respectively. Further increase in β_e leads to gradual increase in $RR_{I_{\text{max}}}$.

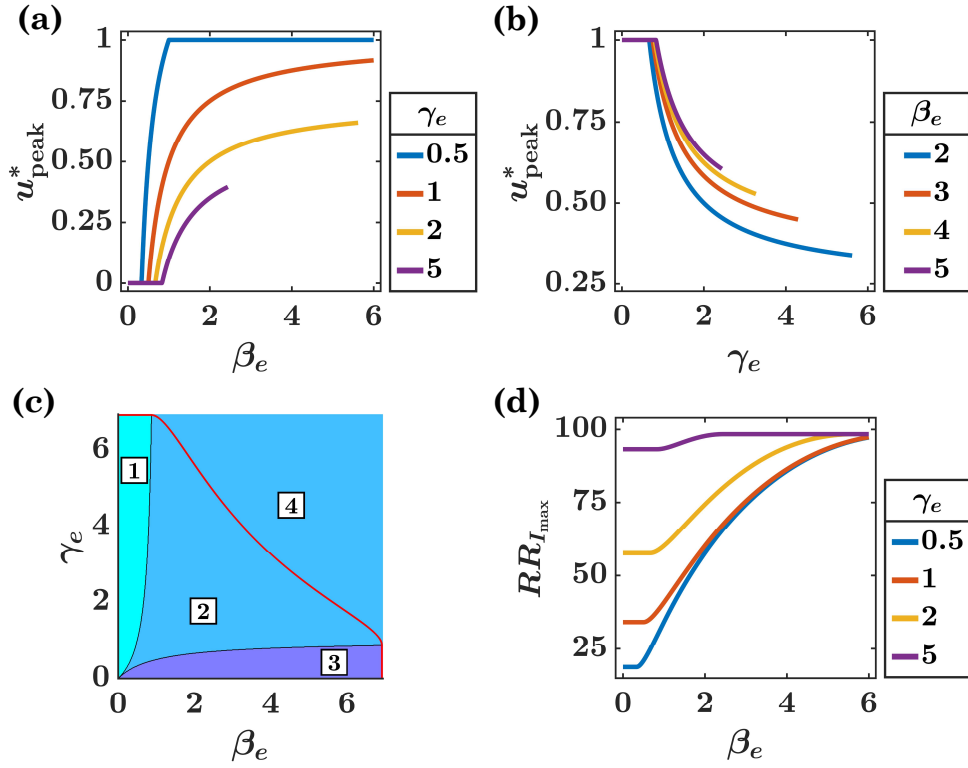


Figure 4: Role of effectiveness parameters in determining the optimal fraction of allocated resources to control disease in an outbreak scenario. Optimal fraction of resources (a) with respect to β_e , (b) with respect to γ_e , (c) when both the effectiveness parameters, β_e and γ_e , are varied simultaneously. The red line represents $S_0 \mathcal{R}_0^{\text{out}} = 1$. Unique u_{peak}^* corresponds to the initial growth of the outbreak size (i.e., $S_0 \mathcal{R}_0^{\text{out}} > 1$; displayed as $\boxed{1}$, $\boxed{2}$ and $\boxed{3}$), while non-unique u_{peak}^* is associated with the initial decay of the outbreak size (i.e., $S_0 \mathcal{R}_0^{\text{out}} < 1$; displayed as $\boxed{4}$). $\boxed{1}$ represents the region where $u_{\text{peak}}^* = 0$, i.e., allocating entire resources toward the recovery-improvement programs is the optimal strategy. $\boxed{3}$ represents the region where the allocation of entire resources towards transmission-reducing programs is the optimal strategy (i.e., $u_{\text{peak}}^* = 1$). $\boxed{2}$ and $\boxed{4}$ represent the regions for resource sharing between two types of intervention programs. u_{peak}^* has a unique value between 0 and 1 in $\boxed{2}$; u_{peak}^* lies within an interval in $\boxed{4}$. (d) Relative reduction of I_{max} with respect to β_e for different values of γ_e .

Impact of delays in resource implementation

In reality, it is quite reasonable to expect a delay between the implementation of intervention measures and the onset of an outbreak due to inap-

propriate information about it at an early stage. To explore the impact of such delays during outbreaks, we calculate the peak of infection (I_{\max}) when the control measures are implemented τ days after the onset of the outbreak (see Fig. 5(a)). We also calculate the percentage of relative increase (RI_{τ}) in the peak of infection for each delay time, τ , compared to the immediate implementation ($\tau = 0$) (see Fig. 5(b)). Lastly, we calculate the corresponding optimal fraction of resources (u_{peak}^*) as a function of delay time, τ , for different values of effectiveness parameters in Fig. 5(c). In our model, for an uncontrolled epidemic (i.e., $\beta_e = \gamma_e = 0$), the infection curve achieves its peak around $t = 19$ days. Since we are interested in peak minimization (lowering the curve of infection), we vary the implementation delay parameter (τ) from days $t = 0$ to $t = 19$.

For lower values of both the effectiveness parameters β_e and γ_e (for instance, $\beta_e = 0.5$ and $\gamma_e = 0.4$), the peak of infection (I_{\max}) remains almost the same until day $\tau = 12$ (see Fig. 5(a), red curve). That means both interventions with lower effectiveness allow a delay of up to 12 days in allocating resources without any significant consequences in terms of the peak of infection. However, if the allocation of resources is delayed further, a gradual increase in the peak of infection can be observed. We find that after a delay of 12 days, RI_{τ} increases gradually and reaches about 17% at day $\tau = 19$ (see Fig. 5(b), red curve) for lower effectiveness parameters. On the other hand, for higher values of both effectiveness parameters (for instance, $\beta_e = 2$ and $\gamma_e = 2$), if the implementation is delayed more than 7 days, a larger increase (approximately 74% at $\tau = 19$; Fig. 5(a)(b), yellow curve) in RI_{τ} is observed compared to the lower effectiveness case. This is because interventions with higher effectiveness are capable of greater reductions in the peak of infection and delays in implementing these interventions lead to a significant relative increase in the same. It is also to be noted that for lower values of effectiveness parameters ($\beta_e = 0.5$ and $\gamma_e = 0.4$), the optimal fraction of resources (u_{peak}^*) remains unchanged with respect to delay (see Fig. 5(c), red curve). This is because u_{peak}^* depends only on β_e and γ_e (see Eq. (9)). Also, for lower values of these effectiveness parameters, the condition, $S_{\tau} \mathcal{R}_0^{\text{out}} > 1$ is satisfied for all τ resulting in a unique optimal value (where S_{τ} denotes the proportion of susceptible individuals for the uncontrolled epidemic at $t = \tau$ day after the onset of the outbreak). For higher values of β_e and γ_e , u_{peak}^* behaves in a slightly different way. Similar to the above-mentioned case, u_{peak}^* stays the same and takes a unique value until a threshold of τ is reached, where

the quantity, $S_\tau \mathcal{R}_0^{\text{out}}$ becomes less or equals to 1 (as susceptible population depletes over time). Consequently, u_{peak}^* becomes non-unique and can take a range of possible values from an interval (see Fig. 5(c), blue and yellow curves).

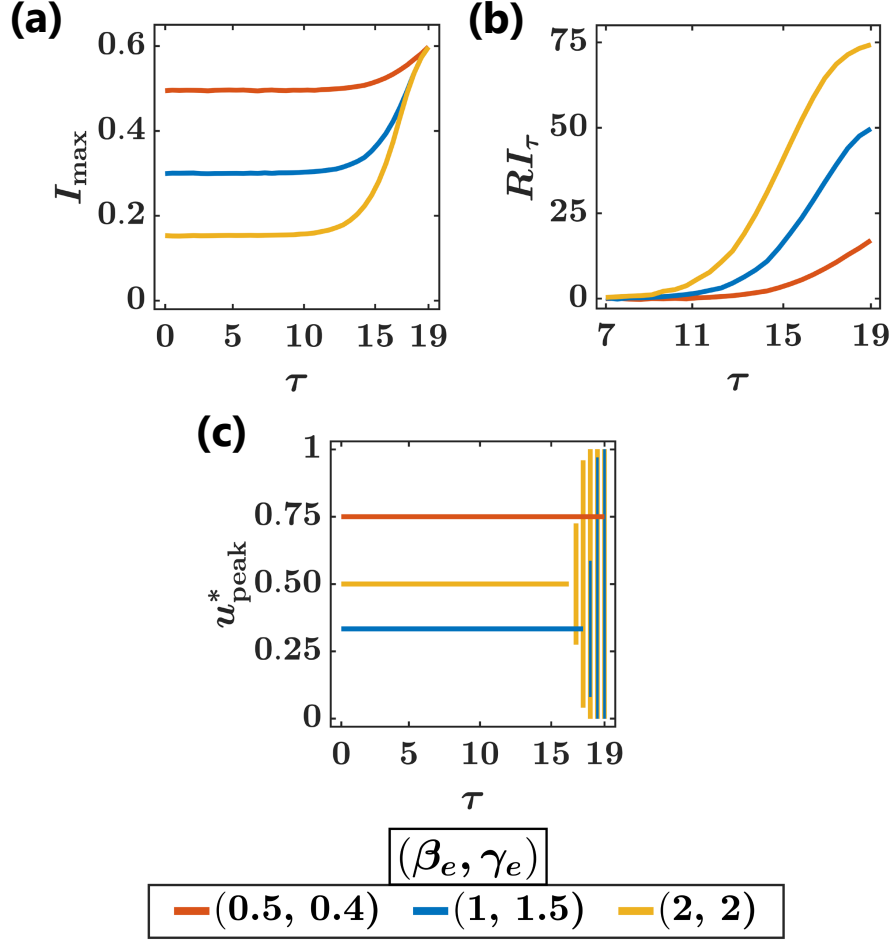


Figure 5: Effect of delay (τ) in implementing interventions during a disease outbreak for different combinations of β_e and γ_e . (a) The peak of infection (I_{max}) as a function of τ . (b) Percentage of the relative increase of I_{max} compared to immediate intervention (i.e., $\tau = 0$) with respect to τ . (c) The optimal fraction of resources (u_{peak}^*) aiming minimization of the peak of infection as a function of delay τ . The vertical lines represent the range of possible values of u_{peak}^* when non-unique.

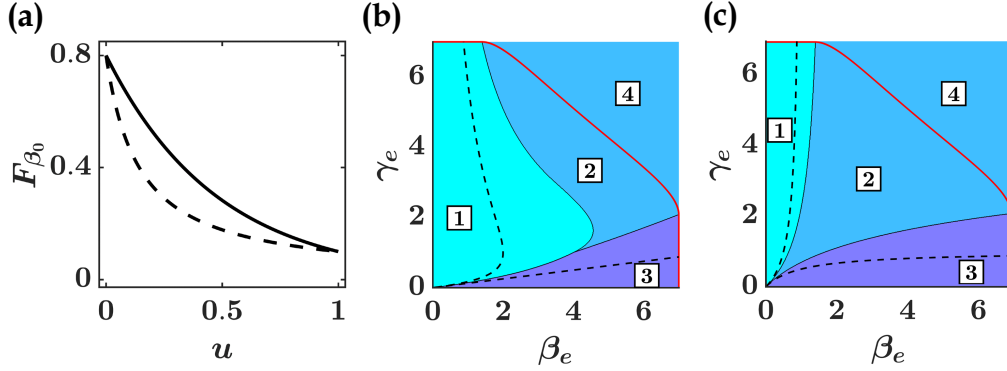


Figure 6: (a) The solid and the dashed lines represent the production functions $F_{\beta_0} = \beta_0 e^{-u \ln(1+\beta_e)}$ and $F_{\beta_0} = \frac{\beta_0}{1+\beta_e u}$ respectively. Role of effectiveness parameters in the optimal fraction of allocated resources to control disease dynamics in (a) long-term and (b) outbreak scenario. Here the red lines, $\mathcal{R}_0^c = 1$ and $S_0 \mathcal{R}_0^{\text{out}} = 1$ in (b) and (c) respectively are shown only for $F_{\beta_0} = \beta_0 e^{-u \ln(1+\beta_e)}$. An increase in [1], [3] are observed compared to the original form in Fig. 3(c) and Fig. 4(c).

3.3. Dependence of resource allocation on production functions

To study the robustness of our results, we choose a different F_{β_0} with decreasing returns given as $F_{\beta_0} = \beta_0 e^{-u \ln(1+\beta_e)}$ (solid line in Fig. 6(a)). A similar exponential function has been used earlier to estimate the production functions for HIV prevention programs (Zaric and Brandeau, 2001; Alistar et al., 2014). For extreme values of u , the new F_{β_0} is equivalent to that assumed in the previous sections (see Fig. 6(a)). As we want to keep the returns to scale type same for better comparison, and since F_{γ_0} exhibits constant returns to scale, it is kept unchanged. This implies that \mathcal{R}_0^c , evaluated at the extreme values of u , are same as in Sec. 3.1. As a result, in the long-term scenario, the line $\mathcal{R}_0^c = 1$, intersects β_e and γ_e axis at the same values as in Fig. 3(c), thereby facilitating comparison. For the outbreak scenario, similar arguments hold for the line, $S_0 \mathcal{R}_0^{\text{out}} = 1$.

We calculate optimal strategies for both long-term and outbreak scenarios for different effectiveness parameters in Fig. 6(b),(c) and compare [1] - [4] with that of Fig. 3(c) and Fig. 4(c). For the long-term case, the non-monotonic behaviour of the β_e^l is retained, which suggests that this property might be independent of the functional forms of F_{β_0} with decreasing returns to scale. On the other hand, for the outbreak scenario, the symmetric nature

of $\boxed{1}$ and $\boxed{3}$ about the line $\beta_e = \gamma_e$ is lost which implies that it can only be true in case of certain production functions. Further, in this case, one can easily note the increase in the area occupied by $\boxed{1}$ and $\boxed{3}$. This signifies a greater possibility that allocating resources to either one of the prevention or treatment programs is the optimal strategy.

Till now, we considered only decreasing and constant returns to scale for transmission-reducing and recovery-improvement programs, respectively. However, it is important to understand the results obtained above in the context of the other returns types of production functions. Hence, in this section, we consider each of $F_{\beta_0}(u)$ and $F_{\gamma_0}(1-u)$ with increasing, constant and decreasing returns to scale and compare the results among all their combinations (see Fig. 7). For a more meaningful comparison between results, we consider that the three types of returns to scale for F_{β_0} (same for F_{γ_0}) are equivalent to each other whenever $u = 0$ or $u = 1$ (see Fig. 2). The exact functional forms for $F_{\beta_0}(u)$ and $F_{\gamma_0}(1-u)$ used in Fig. 7 are described in the caption of Fig. B.10 in Appendix B.

We observe that when F_{β_0} gives either increasing or constant returns to scale and the same holds for F_{γ_0} , the optimal fraction of resources, u_{long}^* takes only extreme values (either 0 in $\boxed{1}$ or 1 in $\boxed{3}$) (see Fig. 7 (a, b, d, e)). Interestingly, in these cases, u_{long}^* is independent of the functional forms of F_{β_0} , F_{γ_0} and has same value for a particular β_e and γ_e (see Proposition. 1, Appendix A). On the other hand, when either or both of F_{β_0} and F_{γ_0} having decreasing returns to scale, u_{long}^* also takes intermediate values between 0 and 1 (see Fig. 7 (c, f-i)). Further, if F_{β_0} (F_{γ_0}) gives decreasing returns to scale and F_{γ_0} (F_{β_0}) changes from increasing to decreasing returns to scale, we observe the region $\boxed{1}$ and $\boxed{3}$ decreases (see Fig. 7 (c, f, i) and (g, h, i)). Moreover, when both intervention programs have decreasing returns to scale, a combined prevention and treatment program is most likely the optimal strategy (see Fig. 7(i)). These results indicate that decreasing returns from investments into the intervention programs promote the necessity for resource sharing. Additionally, moving from increasing to decreasing returns to scale, relatively lower effectiveness of interventions can be sufficient to obtain an asymptotically stable disease-free state, i.e., $\mathcal{R}_0^c < 1$. For instance, when $\beta_e = \gamma_e = 4$, in Fig. 7(g), we have $\mathcal{R}_0^c > 1$ but the same conditions in Fig. 7(i) yield $\mathcal{R}_0^c < 1$. The intuition behind such observation can be easily understood from the shape of the curves, F_{β_0} and F_{γ_0} . When compared to increasing or constant returns, decreasing returns to scale for F_{β_0} , F_{γ_0} implies

that relatively lower transmission and higher recovery rates can be achieved for the same investment (except at $u = 0, 1$). All the results described above also hold true for the outbreak scenario (see Fig. B.10 in Appendix B). It is important to mention that for the long-term scenario, the non-monotonic behaviour of β_e^l with respect to γ_e is observed when at least one of F_{β_0} and F_{γ_0} has decreasing returns to scale (see Fig. 7 (c, f-i)).

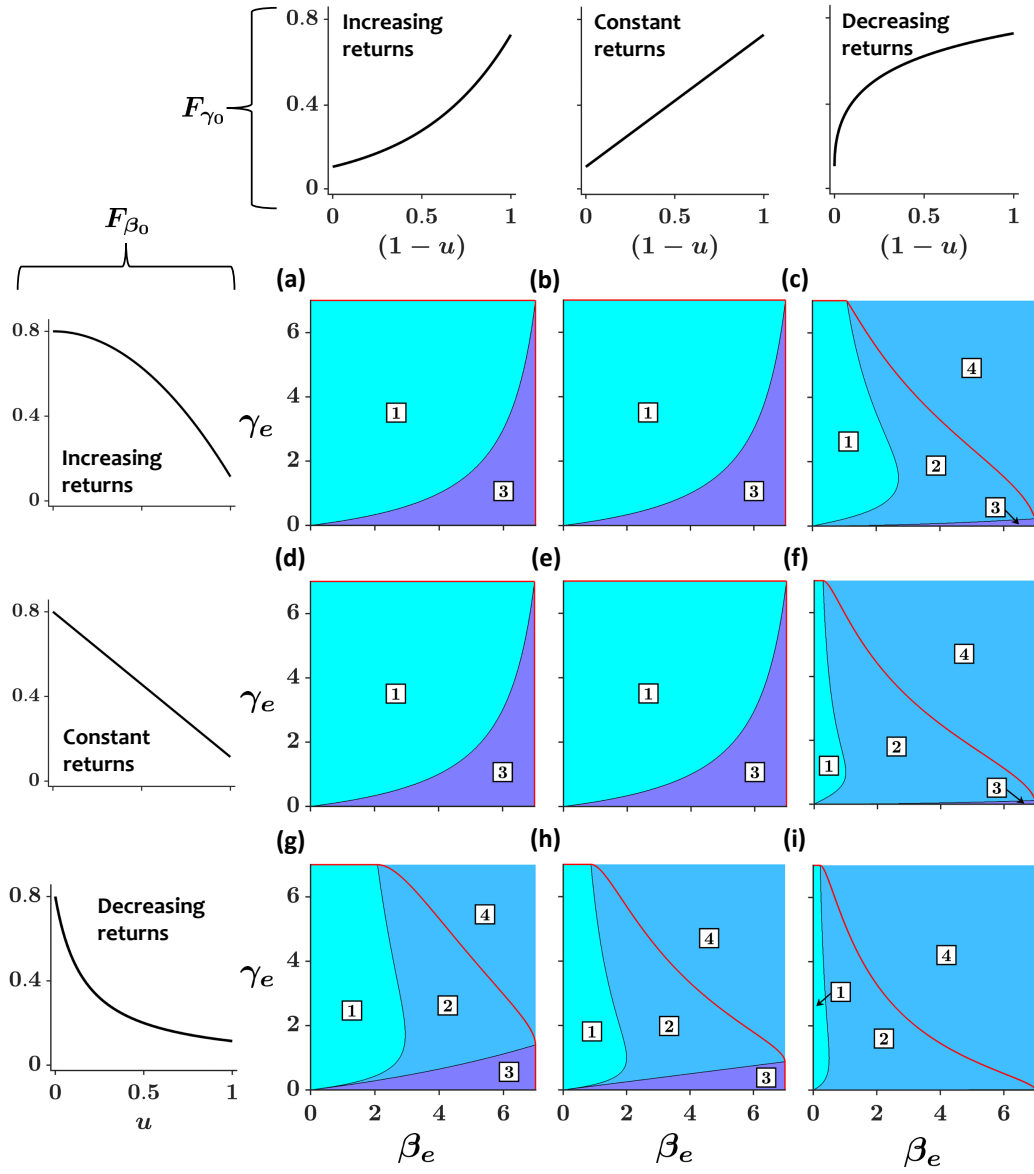


Figure 7: Comparison of the results considering three types of returns to scale for both F_{β_0} and F_{γ_0} to explore the dependence of optimal resource allocation on production functions for control of disease in long-term scenario. The characteristics of u_{long}^* within $\boxed{1}$, $\boxed{2}$, $\boxed{3}$ and $\boxed{4}$ are the same as described in Fig. 3(c). For specific forms of F_{β_0} and F_{γ_0} , refer to Appendix B, Fig. B.10 caption.

4. Discussion

Designing effective intervention strategies is of utmost importance in order to cope with disease outbreaks. Particularly, in low-income countries, resource-constrained situations make it challenging for authorities to allocate resources in an optimal manner to mitigate epidemic scenarios. In this context, the resource allocation trade-off between prevention of transmission and better medical treatment is of significance, yet not well understood. We developed a simple model based on the SIR framework which takes into account production functions for intervention programs and associated effectiveness to address this gap. The interplay between the effectiveness of the two major types of interventions and their implication on optimal resource allocation has been explored under two common epidemic scenarios, viz., long-term and outbreak. While the former case concerns the minimization of the proportion of infected individuals at equilibrium, the primary objective in the later is to minimize the peak of infection during a disease outbreak. For both scenarios, we observe the transitions from allocation of entire resources to only one intervention type to optimal sharing of resources between both types of interventions under different effectiveness parameters settings (Fig. 3(c); Fig. 4(c)). Such behaviour is similar to the threshold-switching of optimal isolation strategy observed in (Hansen and Day, 2011), and also the transition of optimal testing from clinical to mixed strategy noticed in (Calabrese and Demers, 2022).

In the long-term scenario, our results demonstrate that prioritization of transmission-reducing interventions should increase in a monotonic fashion with their effectiveness (Fig. 3(a)). This is suggestive of the fact that in the case of the availability of highly efficient disease prevention measures, it is always advantageous to allocate maximum resources into it. Interestingly, the allocation of recovery-improving interventions does not always behave in the similar way. Due to the constant influx of susceptible populations, there is an increased risk of new infections when prevention programs are less effective. Thus, when treatment programs are sufficiently effective, i.e., beyond a threshold, the optimal solution is to divert some resources to prioritization of prevention programs. However, this non-monotonic behaviour disappears if the prevention programs are sufficiently effective (Fig. 3(b)).

In the outbreak case, our results demonstrate a much simpler optimal resource allocation strategy. In both the transmission-reducing and recovery-improving cases, increasing the effectiveness of an intervention implies the

need to allocate more resources to that intervention measure (Fig. 4). This indicates that allocating more resources towards intervention strategies like symptom monitoring program which was reported to be very effective in preventing diseases like Ebola and SARS (Peak et al., 2017), might prove to be a more fruitful strategy compared to investing in new healthcare facilities during future outbreaks. On the other hand, when treatment programs are highly effective, since the proportion of susceptibles can only decrease over subsequent times, it is unlikely that the risk of new infections will increase. Hence, resources need not be diverted to prioritize prevention programs in such a scenario.

Appropriate allocation of limited resources during the early days of an outbreak is capable of reducing the disease burden. The large change in the relative increase of peak size in the case of more effective control strategies highlights the opportunity to reduce disease burden with the help of timely intervention (Fig. 5(a),(b)). When the intervention measures are less effective, any delay in implementation does not influence the optimal strategy. However, when the interventions are highly effective, although there is a large increase in peak size for too much delay, there can be a wider range of optimal strategies (Fig. 5(c)).

Determining the optimal strategy also requires taking into account the nature of returns from investments into intervention measures. When both the prevention and recovery programs give increasing or constant returns to scale, it is always optimal to invest entire resources into either one of them. On the other hand, decreasing returns from one or both intervention programs increases the likelihood of the optimal strategy being sharing of resources (Fig. 7). This indicates that when the prevention programs concern measures like contact tracing which gives decreasing returns (Armbruster and Brandeau, 2007), a fraction of the resources must also be invested into treatment programs. These findings are comparable to earlier studies on HIV where the allocation strategy "all-or-nothing" in case of increasing and constant, and resource sharing in case of decreasing returns to scale were found to be optimal (Brandeau et al., 2003; Alistar et al., 2014; Brandeau and Zaric, 2009). Additionally, for certain effectiveness of interventions, decreasing returns may help achieve a stable disease-free state or initial decay of outbreak size, which may not be possible otherwise (Fig. 7, Fig. B.10 in Appendix B). This is because decreasing returns to scale imply relatively lower transmission and higher recovery rates for the same investment as compared to the other return types. On increasing effectiveness further, there

is an increased freedom to choose an optimal strategy to drive the system beyond the $\mathcal{R}_0^c = 1$ or $S_0\mathcal{R}_0^{\text{out}} = 1$ line.

Summing up, this work provides a comprehensive understanding of how the effectiveness of different control measures determines the optimal strategy for resource allocation. In spite of our minimalistic approach, our findings provide fundamental insight into the resource allocation problem in case of infectious disease spread. A key limitation of our study is the assumption that increasing investment of resources into intervention programs can alter the transmission and recovery rate instantaneously. However, in reality, that most likely is not the case. Additionally, factors like the number of doctors or success of prevention programs will largely depend on societal conditions which are ignored in this study. Further, while we took into account the different types of production functions to determine the optimal strategies, we did not consider functions which may have decreasing return to scale followed by increasing return to scale or vice versa (Brandeau and Zaric, 2009; Brandeau et al., 2003). Albeit we acknowledge that it is not possible to make recommendations on policy design using a such simple framework, our model does provide a foundational basis on which more specific disease models may be studied in the future. The results highlight the importance of more systematic and involved analyses of the trade-offs between different available strategies by policymakers, especially in developing countries.

Appendix A. Analysis for long-term dynamics

• Calculations for u_{long}^* corresponding to asymptotically stable endemic state:

To control for long-term disease persistence, when there is an asymptotically stable endemic state ($\mathcal{R}_0^c > 1$), we differentiate I^* with respect to u and set it equal to zero. Then after simplifying we obtain u_1 as given in Eq. (4).

At $u = u_1$, we have $\frac{d^2 I^*}{du^2} = \frac{2\mu\beta_e}{\beta_0} \sqrt{\frac{\gamma_0\beta_e\gamma_e}{\beta_0}} > 0$. This shows that I^* is minimum at $u = u_1$.

Since the fraction of allocated resources must be constrained between 0 and 1, from Eq. (4), we have the inequality

$$0 < \beta_e(\gamma_0 + \gamma_0\gamma_e + \mu) - \sqrt{\beta_0\beta_e\gamma_0\gamma_e} < \beta_e\gamma_0\gamma_e. \quad (\text{A.1})$$

For each given γ_e , from the left part of the inequality (A.1), we get a threshold β_e $\left(\beta_e^l = \frac{\beta_0 \gamma_0 \gamma_e}{(\gamma_0 + \gamma_0 \gamma_e + \mu)^2}\right)$ such that if $\beta_e \leq \beta_e^l$, we have $u_{\text{long}}^* = 0$ and if $\beta_e > \beta_e^l$, we have $u_{\text{long}}^* > 0$ (see Fig. 3(a)). Note that β_e^l is non-monotonic in γ_e which we can also visualize in Fig. 3(a) and Fig. 3(c). Moreover, for

$$\beta_e > \beta_e^l, \text{ we get } \frac{\partial u}{\partial \beta_e} = \frac{1}{2} \sqrt{\frac{\beta_0}{\gamma_0 \gamma_e \beta_e^3}} > 0.$$

For each given β_e , from the right part of the inequality (A.1), we get a threshold γ_e $\left(\gamma_e^l = \frac{\beta_e(\gamma_0 + \mu)^2}{\beta_0 \gamma_0}\right)$ such that if $\gamma_e \leq \gamma_e^l$, we get $u_{\text{long}}^* = 1$ and if $\gamma_e > \gamma_e^l$, we get $u_{\text{long}}^* < 1$ (see Fig. 3(b)). Moreover, for $\gamma_e > \gamma_e^l$, we get

$$\frac{\partial u}{\partial \gamma_e} = \frac{1}{2} \sqrt{\frac{\beta_0}{\gamma_0 \beta_e \gamma_e^3} - \frac{\gamma_0 + \mu}{\gamma_0 \gamma_e^2}}. \text{ Now, } \frac{\partial u}{\partial \gamma_e} = 0 \text{ implies } \tilde{\gamma}_e = \frac{4\beta_e(\gamma_0 + \mu)^2}{\beta_0 \gamma_0} \text{ such}$$

that for $\tilde{\gamma}_e > \gamma_e > \gamma_e^l$, we have $\frac{\partial u}{\partial \gamma_e} < 0$ and for $\gamma_e > \tilde{\gamma}_e > \gamma_e^l$, we have

$$\frac{\partial u}{\partial \gamma_e} > 0 \text{ (see Fig. 3(b)).}$$

• **Sensitivity analysis:**

To explore the sensitivity of our findings to the baseline model parameters (β_0 , γ_0 and μ), we vary β_0 from 0.5 to 1.1 day^{-1} , γ_0 from 0.07 to 0.13 day^{-1} , and μ from $\frac{1}{80}$ to $\frac{1}{60}$ $year^{-1}$. Using the Latin Hypercube Sampling scheme, we draw 10,000 samples and obtain 10,000 values of u_{long}^* for a particular β_e , γ_e . Then we plot β_e vs. u_{long}^* (for $\gamma_e = 3$) and γ_e vs. u_{long}^* (for $\beta_e = 4$) with each of the samples (see Fig. A.8).

• **Non-unique u_{long}^* corresponding to the stable disease-free state:**

As the number of infected individuals asymptotically approaches zero whenever $\mathcal{R}_0^c \leq 1$ (Eq. (3)), solving the inequality $\mathcal{R}_0^c \leq 1$ for u will generate the optimal fraction of resources. Using expression of \mathcal{R}_0^c , we have

$$\frac{\beta_0}{(1 + \beta_e u)(\gamma_0(1 + \gamma_e(1 - u)) + \mu)} \leq 1.$$

After simplifying, we get a quadratic inequality of u as

$$Au^2 + Bu + C \leq 0, \text{ where } A = \gamma_0 \gamma_e \beta_e, B = \gamma_0 \gamma_e (1 - \beta_e) - \beta_e (\gamma_0 + \mu), C = \beta_0 - (\gamma_0 + \mu) - \gamma_0 \gamma_e.$$

Now, solving the quadratic inequality, we get an interval for u as

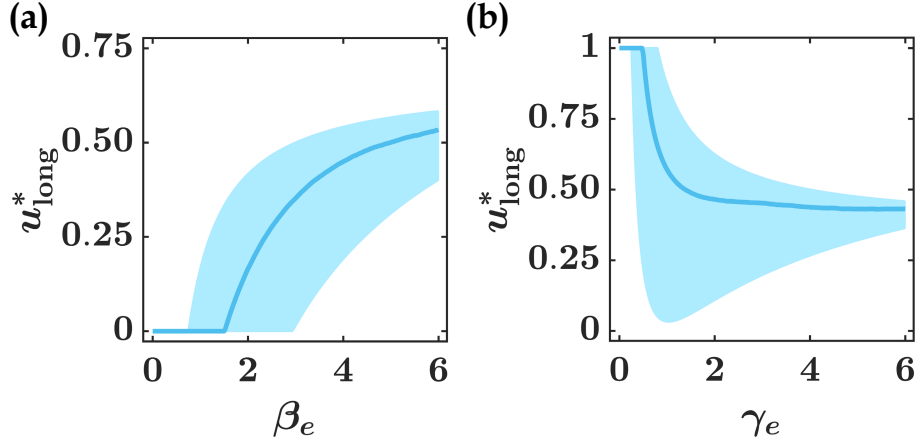


Figure A.8: Sensitivity of (a) β_e vs. u_{long}^* (for $\gamma_e = 3$), (b) γ_e vs. u_{long}^* (for $\beta_e = 4$) to the baseline model parameters. The shaded area represents all the obtained values of u_{long}^* when the baseline parameters are varied: $\beta_0 \in [0.5, 1.1]$, $\gamma_0 \in [0.07, 0.13]$ and $\mu \in [\frac{1}{80}, \frac{1}{60}]$. The solid line represents the median.

$$[u_1, u_2] = \left[\frac{-B - \sqrt{B^2 - 4AC}}{2A}, \frac{-B + \sqrt{B^2 - 4AC}}{2A} \right]$$

Since the fraction of allocated resources must be constrained between 0 and 1, we have the optimal fraction of resources corresponding to $\mathcal{R}_0^c \leq 1$ lies within

$$[u_{11}, u_{12}] = [u_1, u_2] \cap [0, 1] \quad (\text{A.2})$$

Selecting any $u \in [u_{11}, u_{12}]$ would give $\mathcal{R}_0^c \leq 1$ (as $[u_{11}, u_{12}] \subseteq [u_1, u_2]$), and consequently from Eq. (3) we have $I^* = 0$. Conversely, $I^* = 0$ implies $\mathcal{R}_0^c \leq 1$, and consequently $u \in [u_{11}, u_{12}]$. That means the interior points of the interval (A.2) are the values of u_{long}^* for which $I^* = 0$ with particular β_e, γ_e . That is why u_{long}^* is not unique within $\boxed{4}$ in Fig. 3(c).

Additionally, for specific β_e and γ_e , in Fig. A.9, we display unique and non-unique u_{long}^* to control long-term disease persistence associated with both the stable equilibria states.

Proposition 1. *For the resource allocation in long-term disease dynamics scenario, if both F_{β_0} and F_{γ_0} are with increasing or constant returns to scale or one with increasing and the other constant returns to scale, the optimal*

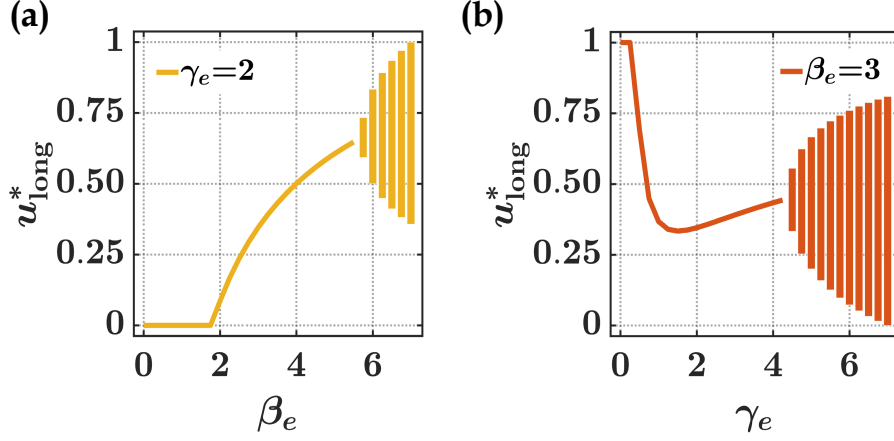


Figure A.9: The unique and non-unique optimal fraction of resources (u_{long}^*) given by Eq. (5) for the case of long-term disease dynamics. The vertical lines denote the range of possible values for u_{long}^* in the non-unique case. Here unique u_{long}^* corresponds to $\boxed{1}$, $\boxed{2}$ and $\boxed{3}$ while non-unique u_{long}^* corresponds to $\boxed{4}$ in Fig. 3(c). (a) β_e vs. u_{long}^* for $\gamma_e = 2$ and (b) γ_e vs. u_{long}^* for $\beta_e = 3$. Rest of the parameters are taken from Table 1.

fraction of resource u_{long}^ only takes the extreme values (either 0 or 1) within the region of the asymptotically stable endemic state. Moreover, u_{long}^* must be the same in all these cases for a given β_e, γ_e .*

Proof: In general, during the control of long-term dynamics of disease with any type of returns to scale for F_{β_0} and F_{γ_0} , from Eq. (3) we have

$$I^* = \mu \left(\frac{1}{(F_{\gamma_0} + \mu)} - \frac{1}{F_{\beta_0}} \right) \quad \left(\text{as } \mathcal{R}_0^c = \frac{F_{\beta_0}}{F_{\gamma_0} + \mu} \right)$$

corresponding to an asymptotically stable endemic state ($\mathcal{R}_0^c > 1$). Here both $F_{\beta_0}, F_{\gamma_0}$ are differentiable on $(0, 1)$ and $F_{\beta_0}, F_{\gamma_0} \neq 0$ on $[0, 1]$. Consequently, I^* is also differentiable on $(0, 1)$.

Now, differentiating I^* with respect to u we have

$$I^{*'} = \mu \left(\frac{F'_{\beta_0}(F_{\gamma_0} + \mu)^2 - F'_{\gamma_0}(F_{\beta_0})^2}{(F_{\beta_0})^2(F_{\gamma_0} + \mu)^2} \right), \quad (\text{A.3})$$

and

$$I^{*''} = \mu \left(\frac{2(F'_{\gamma_0})^2}{(F_{\gamma_0} + \mu)^3} - \frac{2(F'_{\beta_0})^2}{(F_{\beta_0})^3} - \frac{F''_{\gamma_0}}{(F_{\gamma_0} + \mu)^2} + \frac{F''_{\beta_0}}{(F_{\beta_0})^2} \right). \quad (\text{A.4})$$

• **Case-1: Both the production functions F_{β_0} and F_{γ_0} with constant returns to scale**

As $F_{\beta_0}(u)$ has constant returns to scale, then $F_{\beta_0}(u)$ is linearly decreasing function of u (i.e., $F'_{\beta_0} < 0$ and $F''_{\beta_0} = 0$). Also, since $F_{\gamma_0}(1-u)$ has constant returns to scale, $F_{\gamma_0}(1-u)$ is linearly increasing function of $(1-u)$, and equivalently, F_{γ_0} is linearly decreasing function of u (i.e., $F'_{\gamma_0} < 0$ and $F''_{\gamma_0} = 0$).

It is to be noted that we denote I^* as I_{CC}^* when both production functions yield constant returns to scale. From Eq. (A.4), we have

$$I_{CC}^{*''} = 2\mu \left(\frac{(F'_{\gamma_0})^2}{(F_{\gamma_0} + \mu)^3} - \frac{(F'_{\beta_0})^2}{(F_{\beta_0})^3} \right).$$

If I_{CC}^* is convex on any subinterval S of $[0, 1]$ (i.e., $I_{CC}^{*''} \geq 0$ for all $u \in S \subseteq [0, 1]$), then we have

$$\begin{aligned} \frac{F'_{\gamma_0}}{F'_{\beta_0}} &\geq \left(\frac{F_{\gamma_0} + \mu}{F_{\beta_0}} \right)^{3/2} \\ \implies (\mathcal{R}_0^c)^{3/2} F'_{\gamma_0} &\leq F'_{\beta_0}, \text{ for all } u \in S, \end{aligned} \quad (\text{A.5})$$

because $F'_{\beta_0} < 0$ and $F'_{\gamma_0} < 0$.

Now, for all $u \in S \subseteq [0, 1]$,

$$\begin{aligned} &F'_{\beta_0}(F_{\gamma_0} + \mu)^2 - F'_{\gamma_0}(F_{\beta_0})^2 \\ &\geq (\mathcal{R}_0^c)^{3/2} F'_{\gamma_0}(F_{\gamma_0} + \mu)^2 - F'_{\gamma_0}(F_{\beta_0})^2 \\ &\quad \text{(using Eq. (A.5))} \\ &= (-F'_{\gamma_0})(F_{\gamma_0} + \mu)^2 \left(\frac{(F_{\beta_0})^2}{(F_{\gamma_0} + \mu)^2} - (\mathcal{R}_0^c)^{3/2} \right) \\ &= (-F'_{\gamma_0})(F_{\gamma_0} + \mu)^2 \left((\mathcal{R}_0^c)^2 - (\mathcal{R}_0^c)^{3/2} \right) \\ &> 0 \quad (\text{as } F'_{\gamma_0} < 0, \mathcal{R}_0^c > 1) \end{aligned} \quad (\text{A.6})$$

From Eq. (A.3) we have $I_{CC}^{*'} \geq 0$ for all $u \in S \subseteq [0, 1]$. So, we get I_{CC}^* as an increasing function of u on $S \subseteq [0, 1]$ whenever I_{CC}^* is convex on $S \subseteq [0, 1]$.

Thus if I_{CC}^* is convex on a subinterval of $[0, 1]$, then I_{CC}^* must be increasing on that subinterval. Also, it is worth mentioning that I_{CC}^* may be convex or concave entirely on $[0, 1]$. In that case, it is obvious to see that I_{CC}^* attains its minimum either at 0 and 1. Moreover, there may be situations where I_{CC}^* is first convex on a certain subinterval and then concave on the rest of the subinterval of $[0, 1]$. It is important to point out that if I_{CC}^* is first concave on a certain subinterval of $[0, 1]$, then it cannot be further convex on the remaining subinterval of $[0, 1]$. Otherwise, there must be a cusp point of I_{CC}^* within $(0, 1)$ where I_{CC}^* fails to be differentiable, which would contradict the differentiability of I_{CC}^* on $(0, 1)$.

Here we are trying to minimize I_{CC}^* over the interval $[0, 1]$. If I_{CC}^* is convex entirely on $[0, 1]$, then I_{CC}^* must attain its minimum value at 0 as I_{CC}^* increases over $[0, 1]$ in that case. If I_{CC}^* is concave entirely on $[0, 1]$ or first convex on a certain subinterval and then concave on the remaining subinterval of $[0, 1]$, then I_{CC}^* must achieve its minimum value either at 0 (if $I_{CC}^*(u)|_{u=0} < I_{CC}^*(u)|_{u=1}$) or 1 (if $I_{CC}^*(u)|_{u=0} > I_{CC}^*(u)|_{u=1}$). If possible let I_{CC}^* attain its minimum value at a point $u = c$ other than 0, 1, so $c \in (0, 1)$.

Since I_{CC}^* is minimum at $u = c \in (0, 1)$ and I_{CC}^* is differentiable on $(0, 1)$, then the following must hold in a certain neighborhood of c :

$$I_{CC}^{*'}(u) = \begin{cases} < 0 & \text{as } u \rightarrow c^- \\ 0 & \text{at } u = c \\ > 0 & \text{as } u \rightarrow c^+. \end{cases}$$

This means that there must be a certain neighborhood of c at which I_{CC}^* becomes convex and non-monotonic. This contradicts the fact that I_{CC}^* must increase if convex. Thus our assumption is incorrect and I_{CC}^* cannot attain its minimum value at any point $c \in (0, 1)$. Consequently, I_{CC}^* attains minimum value only at 0 or 1. Therefore, u_{long}^* only takes the extreme values (either 0 or 1) within the region of the asymptotically stable endemic state.

• Case-2: Both the production functions F_{β_0} and F_{γ_0} with increasing returns to scale

As both $F_{\beta_0}(u)$ and $F_{\gamma_0}(1 - u)$ have increasing returns to scale, then $F_{\beta_0}(u)$ is concave (concave down) and decreasing function of u (i.e., $F_{\beta_0}' < 0$ and $F_{\beta_0}'' \leq 0$). Also, $F_{\gamma_0}(1 - u)$ is convex (concave up) and increasing function of $(1 - u)$, equivalently, F_{γ_0} is convex and decreasing function of u (i.e., $F_{\gamma_0}' < 0$

and $F''_{\gamma_0} \geq 0$).

Here we denote I^* as I_{II}^* when both production functions yield increasing returns. From Eq. (A.4), we have

$$\begin{aligned} I_{\text{II}}^{*''} &= \mu \left(\frac{2(F'_{\gamma_0})^2}{(F_{\gamma_0} + \mu)^3} - \frac{2(F'_{\beta_0})^2}{(F_{\beta_0})^3} - \frac{F''_{\gamma_0}}{(F_{\gamma_0} + \mu)^2} + \frac{F''_{\beta_0}}{(F_{\beta_0})^2} \right) \\ &\leq 2\mu \left(\frac{(F'_{\gamma_0})^2}{(F_{\gamma_0} + \mu)^3} - \frac{(F'_{\beta_0})^2}{(F_{\beta_0})^3} \right). \end{aligned}$$

With similar arguments as Eq. (A.5), Eq. (A.6) in case-1, here we can prove that I_{II}^* is increasing in u whenever I_{II}^* is convex, and consequently, u_{long}^* only takes the extreme values (either 0 or 1) within $\mathcal{R}_0^c > 1$.

• **Case-3: One of the production functions F_{β_0} and F_{γ_0} with increasing and the other with constant returns to scale**

First, we consider that $F_{\beta_0}(u)$ and $F_{\gamma_0}(1-u)$ have increasing and constant returns to scale respectively. Then we have $F'_{\beta_0} < 0$, $F''_{\beta_0} \leq 0$, $F'_{\gamma_0} < 0$ and $F''_{\gamma_0} = 0$.

Here we denote I^* as I_{IC}^* for F_{β_0} and F_{γ_0} with increasing and constant returns to scale respectively. From Eq. (A.4), we have

$$\begin{aligned} I_{\text{IC}}^{*''} &= \mu \left(\frac{2(F'_{\gamma_0})^2}{(F_{\gamma_0} + \mu)^3} - \frac{2(F'_{\beta_0})^2}{(F_{\beta_0})^3} + \frac{F''_{\beta_0}}{(F_{\beta_0})^2} \right) \\ &\leq 2\mu \left(\frac{(F'_{\gamma_0})^2}{(F_{\gamma_0} + \mu)^3} - \frac{(F'_{\beta_0})^2}{(F_{\beta_0})^3} \right). \end{aligned}$$

Likewise, we have

$$\begin{aligned} I_{\text{CI}}^{*''} &= \mu \left(\frac{2(F'_{\gamma_0})^2}{(F_{\gamma_0} + \mu)^3} - \frac{2(F'_{\beta_0})^2}{(F_{\beta_0})^3} - \frac{F''_{\gamma_0}}{(F_{\gamma_0} + \mu)^2} \right) \\ &\leq 2\mu \left(\frac{(F'_{\gamma_0})^2}{(F_{\gamma_0} + \mu)^3} - \frac{(F'_{\beta_0})^2}{(F_{\beta_0})^3} \right). \end{aligned}$$

In this case, also using similar arguments as Eq. (A.5), Eq. (A.6) in case-1, it can be shown that u_{long}^* only takes the extreme values either 0 or 1 within

$\mathcal{R}_0^c > 1$.

Here we consider three types of returns to scale for F_{β_0} (and F_{γ_0}) which have identical values at extreme point 0 or 1 for certain β_e, γ_e (i.e., three return types for F_{β_0} (and F_{γ_0}) are equivalent to each other whenever $u = 0$ or $u = 1$). This is why the value of the objective function, I^* with any type of returns to scale related to F_{β_0} and F_{γ_0} must be identical at the two extreme points for a given β_e and γ_e . Since u_{long}^* only takes extreme values within $\mathcal{R}_0^c > 1$, u_{long}^* must be the same in all these cases described above for a given β_e, γ_e . For this reason, regions $\boxed{1}$, $\boxed{3}$ in the corresponding sub-figures ((a), (b), (d), (e)) in Fig. 7 are identical.

Appendix B. Analysis for outbreak scenario

• Derivation of the epidemic peak (I_{max}) :

From the first two equations of the outbreak model (i.e., model (2) with $\mu = 0$) we get

$$dI/dt = \left(-1 + \frac{1}{S(t)\mathcal{R}_0^{\text{out}}} \right) dS/dt. \quad (\text{B.1})$$

We know that $dS/dt < 0$ at all times in the outbreak scenario for non-zero initial infection sizes ($I_0 = I(0)$). Then from Eq. (B.1), we observe that dI/dt is initially greater than, equal to, or less than zero when $S_0\mathcal{R}_0^{\text{out}}$ is greater than, equal to, or less than one, respectively. Thus the outbreak is initially in a growing, stationary, or decaying state when $S_0\mathcal{R}_0^{\text{out}}$ is greater than, equal to, or less than one, respectively. Also, if $dI/dt < 0$ at some time t_1 , then $dI/dt < 0$ at any later time t_2 . This means, if the outbreak size begins to decay at any time, it continues to decay for all subsequent periods. Now, integrating the above Eq. (B.1) and using the initial condition we get

$$I(t) = I_0 + S_0 - S(t) + \frac{1}{\mathcal{R}_0^{\text{out}}} \ln \frac{S(t)}{S_0}.$$

Now, if the outbreak is initially in a growing or stationary state ($S_0\mathcal{R}_0^{\text{out}} \geq 1$), during the peak of the epidemic (let the peak be reached at $t = t_{\text{peak}}$), the rate at which individuals are infected becomes zero (i.e., $dI/dt = 0$ at

$t = t_{\text{peak}}$). Then from Eq. (B.1), we get $S(t_{\text{peak}}) = \frac{1}{\mathcal{R}_0^{\text{out}}}$ (i.e., the fraction of susceptible is equal to the reciprocal of control reproduction number similar as in (Keeling and Rohani, 2011)).

Thus from above equation, we obtain the epidemic peak

$$I_{\text{max}} = I(t_{\text{peak}}) = S_0 + I_0 - \frac{\left(\ln \left(S_0 \mathcal{R}_0^{\text{out}} \right) + 1 \right)}{\mathcal{R}_0^{\text{out}}}. \quad (\text{B.2})$$

From the above expression, we have $I_{\text{max}} = I_0$ for the special case $S_0 \mathcal{R}_0^{\text{out}} = 1$. Also, for $S_0 \mathcal{R}_0^{\text{out}} < 1$, we must have $I_{\text{max}} = I_0$ because $dI/dt < 0$ at all times. Finally, the expression for the epidemic peak related to several initial states of the outbreak size is given by Eq. (7).

• **Derivation of u_{peak}^* corresponding to initial growth of the outbreak size :**

For the outbreak scenarios, when the outbreak is initially in a growing state ($S_0 \mathcal{R}_0^{\text{out}} > 1$), resources are distributed in such a way that the epidemic peak (I_{max}) will be minimum. Differentiating I_{max} with respect to u and after simplification we have

$$\frac{dI_{\text{max}}}{du} = \frac{\ln(S_0 \mathcal{R}_0^{\text{out}})}{\left(\mathcal{R}_0^{\text{out}}\right)^2} \frac{d\mathcal{R}_0^{\text{out}}}{du}.$$

Equating it to zero and simplifying we obtain $u_p = \frac{1}{2} \left(1 - \frac{1}{\beta_e} + \frac{1}{\gamma_e} \right)$. At $u = u_p$, we have $\frac{d^2 I_{\text{max}}}{du^2} = \frac{2\gamma_0 \beta_e \gamma_e}{\beta_0} \ln(S_0 \mathcal{R}_0^{\text{out}}) > 0$. This shows that I_{max} is minimum at $u = u_p$.

• **Effect of β_e, γ_e on u_{peak}^* during the initial growth of the outbreak state (i.e., within $S_0 \mathcal{R}_0^{\text{out}} > 1$) :**

For extremely lower β_e , u_{peak}^* tends to 0 and for extremely lower γ_e , u_{peak}^* tends to 1 respectively. Also, since the fraction of allocated resources must be constrained between 0 and 1, from Eq. (8), we have the inequality

$$-\beta_e \gamma_e < \beta_e - \gamma_e < \beta_e \gamma_e. \quad (\text{B.3})$$

For each given γ_e , from the left part of the inequality (B.3), we get a threshold $\beta_e \left(\beta_e^p = \frac{\gamma_e}{1 + \gamma_e} \right)$ such that if $\beta_e \leq \beta_e^p$, we have $u_{\text{peak}}^* = 0$ and if $\beta_e > \beta_e^p$, we have $u_{\text{peak}}^* > 0$ (see Fig. 4(a)). Moreover, for $\beta_e > \beta_e^p$, we get $\frac{\partial u_p}{\partial \beta_e} = \frac{1}{2\beta_e^2} > 0$. For each given β_e , from the right part of the inequality (B.3), we get a threshold $\gamma_e \left(\gamma_e^p = \frac{\beta_e}{1 + \beta_e} \right)$ such that if $\gamma_e \leq \gamma_e^p$, we get $u_{\text{peak}}^* = 1$ and if $\gamma_e > \gamma_e^p$, we get $u_{\text{peak}}^* < 1$ (see Fig. 4(b)). Moreover, for $\gamma_e > \gamma_e^p$, we get $\frac{\partial u_p}{\partial \gamma_e} = -\frac{1}{2\gamma_e^2} < 0$.

Now, from the expression for u_p , we have the following relationship between u_{peak}^* and $(1 - u_{\text{peak}}^*)$ for all β_e, γ_e as

$$u_{\text{peak}}^*(\beta_e, \gamma_e) = 1 - u_{\text{peak}}^*(\gamma_e, \beta_e).$$

$$\text{i.e., } u_{\text{peak}}^*(\beta_e, \gamma_e) + u_{\text{peak}}^*(\gamma_e, \beta_e) = 1.$$

Utilizing the fact $u_{\text{peak}}^* = \frac{1}{2}$ for each $\beta_e = \gamma_e$, from above relation we can observe that u_{peak}^* partitioned the parameter space of β_e, γ_e into two parts along the line $\beta_e = \gamma_e$ such that within the parameter space $\{(\beta_e, \gamma_e) : \beta_e > \gamma_e\}$, we get $u_{\text{peak}}^* > \frac{1}{2}$, on the other hand, $u_{\text{peak}}^* < \frac{1}{2}$ within $\{(\beta_e, \gamma_e) : \beta_e < \gamma_e\}$. So we can conclude that u_{peak}^* show symmetric behaviour about the line $\beta_e = \gamma_e$ within the parameter space of β_e, γ_e during initial growth of the outbreak size.

• **Non-unique u_{peak}^* corresponding to the initial decay of the outbreak size:**

Since the outbreak is initially in a stationary or decaying state (i.e., $I_{\text{max}} = I_0$) according to $S_0 \mathcal{R}_0^{\text{out}} = 1$ or $S_0 \mathcal{R}_0^{\text{out}} < 1$ respectively, solving the inequality $S_0 \mathcal{R}_0^{\text{out}} \leq 1$ for u would generate the optimal fraction of resources. Using the expression of $\mathcal{R}_0^{\text{out}}$ we have

$$\frac{S_0 \beta_0}{\gamma_0 (1 + \beta_e u) (1 + \gamma_e (1 - u))} \leq 1.$$

Simplifying algebraically we get a quadratic inequality of u as $Au^2 + Bu + C \leq 0$. Here $A = \beta_e \gamma_e$, $B = \gamma_e - \beta_e - \beta_e \gamma_e$ and $C = \frac{S_0 \beta_0}{\gamma_0} - \gamma_e - 1$. Now, solving the quadratic inequality, we get an interval for u as

$$[u_a, u_b] = \left[\frac{-B - \sqrt{B^2 - 4AC}}{2A}, \frac{-B + \sqrt{B^2 - 4AC}}{2A} \right]$$

Since the fraction of allocated resources must be constrained between 0 and 1, we have the optimal fraction of resources corresponding to $S_0\mathcal{R}_0^{\text{out}} \leq 1$ lies within

$$[u_{p_1}, u_{p_2}] = [u_a, u_b] \cap [0, 1] \quad (\text{B.4})$$

Selecting any $u \in [u_{p_1}, u_{p_2}]$ would give $S_0\mathcal{R}_0^{\text{out}} \leq 1$ (as $[u_{p_1}, u_{p_2}] \subseteq [u_a, u_b]$), and consequently from Eq. (7) we have $I_{\text{max}} = I_0$ (i.e., the outbreak being unable to grow initially). Conversely, $I_{\text{max}} = I_0$ implies $S_0\mathcal{R}_0^{\text{out}} \leq 1$, and consequently $u \in [u_{p_1}, u_{p_2}]$. That means the interior points of the interval (B.4) are the values of u_{peak}^* for which $I_{\text{max}} = I_0$ with particular β_e, γ_e . That is why u_{peak}^* is not unique within $\boxed{4}$ in Fig. 4(c).

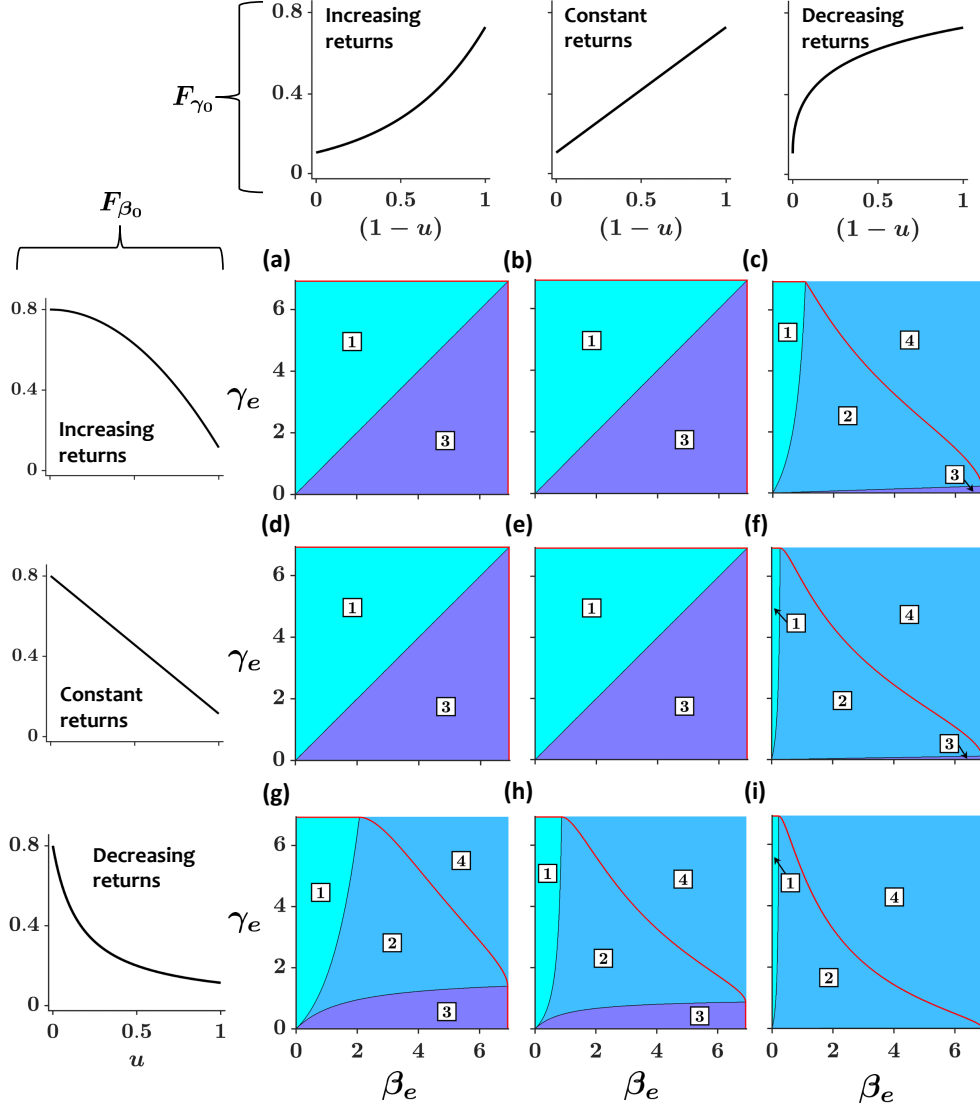


Figure B.10: Comparison of the results considering three types of returns to scale for both F_{β_0} and F_{γ_0} to explore the dependence of optimal resource allocation on production functions for control of disease in an outbreak scenario. The characteristics of u_{peak}^* within $\boxed{1}$, $\boxed{2}$, $\boxed{3}$ and $\boxed{4}$ are the same as described in Fig. 4(c). Functional forms for F_{β_0} with three types of returns to scale are given as follows: $F_{\beta_0} = \beta_0 \left(1 - \frac{\beta_e u^2}{1 + \beta_e}\right)$ (increasing returns to scale), $\beta_0 \left(1 - \frac{\beta_e u}{1 + \beta_e}\right)$ (constant returns to scale), and $\frac{\beta_0}{1 + \beta_e u}$ (decreasing returns to scale). Also, Functional forms for F_{γ_0} with three types of returns to scale are given as follows: $F_{\gamma_0} = \gamma_0 (1 + \gamma_e)^{(1-u)}$ (increasing returns to scale), $\gamma_0 (1 + \gamma_e (1-u))$ (constant returns to scale), and $\gamma_0 \left(1 + \frac{2\gamma_e \sqrt{(1-u)}}{1 + \sqrt{(1-u)}}\right)$ (decreasing returns to scale).

Author's contribution

B. M.: Methodology, Formal analysis, Software, Writing - original draft, Writing - review & editing. **S. B.:** Conceptualization, Methodology, Supervision, Writing - review & editing. **A. S.:** Conceptualization, Methodology, Supervision, Writing - review & editing. **J. C.:** Supervision, Conceptualization, Writing - review & editing.

Acknowledgements

B. M. is supported by Junior Research Fellowship from University Grants Commission (UGC), India. A. S. and S. B. would like to acknowledge Senior Research Fellowship from CSIR, India for funding them during the initial part of this work. A.S. is also partially funded by the Center of Advanced Systems Understanding (CASUS), which is financed by Germany's Federal Ministry of Education and Research (BMBF) and by the Saxon Ministry for Science, Culture and Tourism (SMWK) with tax funds on the basis of the budget approved by the Saxon State Parliament. S.B. was supported by the Visiting Scientist fellowship at Indian Statistical Institute, Kolkata during a part of this work. S.B. would also like to acknowledge his present funding under the Marie Skłodowska–Curie grant agreement 101025056 for the project 'SpatialSAVE'.

References

- Adhikari, S.P., Meng, S., Wu, Y.J., Mao, Y.P., Ye, R.X., Wang, Q.Z., Sun, C., Sylvia, S., Rozelle, S., Raat, H., et al., 2020. Epidemiology, causes, clinical manifestation and diagnosis, prevention and control of coronavirus disease (COVID-19) during the early outbreak period: a scoping review. *Infectious Diseases of Poverty* 9, 1–12.
- Alistar, S.S., Long, E.F., Brandeau, M.L., Beck, E.J., 2014. HIV epidemic control—a model for optimal allocation of prevention and treatment resources. *Health Care Management Science* 17, 162–181.
- Anderson, R.M., May, R.M., 1992. *Infectious diseases of humans: dynamics and control*. Oxford university press.
- Angulo, M.T., Castaños, F., Moreno-Morton, R., Velasco-Hernández, J.X., Moreno, J.A., 2021. A simple criterion to design optimal non-pharmaceutical interventions for mitigating epidemic outbreaks. *Journal of the Royal Society Interface* 18, 20200803.

- Armbruster, B., Brandeau, M.L., 2007. Contact tracing to control infectious disease: when enough is enough. *Health care management science* 10, 341–355.
- Beigel, J.H., Tomashek, K.M., Dodd, L.E., Mehta, A.K., Zingman, B.S., Kalil, A.C., Hohmann, E., Chu, H.Y., Luetkemeyer, A., Kline, S., et al., 2020. Remdesivir for the treatment of covid-19. *New England Journal of Medicine* 383, 1813–1826.
- Benson, C.A., Brooks, J.T., Holmes, K.K., Kaplan, J.E., Masur, H., Pau, A., 2009. Guidelines for prevention and treatment opportunistic infections in HIV-infected adults and adolescents; recommendations from cdc, the national institutes of health, and the HIV medicine association/infectious diseases society of america .
- Bolzoni, L., Bonacini, E., Della Marca, R., Groppi, M., 2019. Optimal control of epidemic size and duration with limited resources. *Mathematical Biosciences* 315, 108232.
- Brandeau, M.L., Zaric, G.S., 2009. Optimal investment in hiv prevention programs: more is not always better. *Health care management science* 12, 27–37.
- Brandeau, M.L., Zaric, G.S., De Angelis, V., 2005. Improved allocation of hiv prevention resources: using information about prevention program production functions. *Health Care Management Science* 8, 19–28.
- Brandeau, M.L., Zaric, G.S., Richter, A., 2003. Resource allocation for control of infectious diseases in multiple independent populations: beyond cost-effectiveness analysis. *Journal of health economics* 22, 575–598.
- Breda, D., Diekmann, O., De Graaf, W., Pugliese, A., Vermiglio, R., 2012. On the formulation of epidemic models (an appraisal of Kermack and McKendrick). *Journal of Biological Dynamics* 6, 103–117.
- Calabrese, J.M., Demers, J., 2022. How optimal allocation of limited testing capacity changes epidemic dynamics. *Journal of Theoretical Biology* 538, 111017.

- Colizza, V., Barrat, A., Barthélemy, M., Vespignani, A., 2007. Predictability and epidemic pathways in global outbreaks of infectious diseases: the SARS case study. *BMC Medicine* 5, 1–13.
- Deka, A., Bhattacharyya, S., 2019. Game dynamic model of optimal budget allocation under individual vaccination choice. *Journal of Theoretical Biology* 470, 108–118.
- Emanuel, E.J., Persad, G., Upshur, R., Thome, B., Parker, M., Glickman, A., Zhang, C., Boyle, C., Smith, M., Phillips, J.P., 2020. Fair allocation of scarce medical resources in the time of COVID-19. *New England Journal of Medicine* 382, 2049–2055.
- Farmer, P., 2001. The major infectious diseases in the world—to treat or not to treat? *New England Journal of Medicine* 345, 208–210.
- Fraser, C., Donnelly, C.A., Cauchemez, S., Hanage, W.P., Van Kerkhove, M.D., Hollingsworth, T.D., Griffin, J., Baggaley, R.F., Jenkins, H.E., Lyons, E.J., et al., 2009. Pandemic potential of a strain of influenza A (H1N1): early findings. *Science* 324, 1557–1561.
- Ghosh, S., Senapati, A., Chattopadhyay, J., Hens, C., Ghosh, D., 2021. Optimal test-kit-based intervention strategy of epidemic spreading in heterogeneous complex networks. *Chaos: An Interdisciplinary Journal of Nonlinear Science* 31, 071101.
- Gostin, L.O., 2014. Ebola: towards an international health systems fund. *The Lancet* 384, e49–e51.
- Gostin, L.O., Friedman, E.A., 2015. A retrospective and prospective analysis of the west african ebola virus disease epidemic: robust national health systems at the foundation and an empowered who at the apex. *The Lancet* 385, 1902–1909.
- Group, R.C., 2020. Effect of hydroxychloroquine in hospitalized patients with covid-19. *New England Journal of Medicine* 383, 2030–2040.
- Gubler, D.J., 2002. Epidemic dengue/dengue hemorrhagic fever as a public health, social and economic problem in the 21st century. *Trends in microbiology* 10, 100–103.

- Hansen, E., Day, T., 2011. Optimal control of epidemics with limited resources. *Journal of Mathematical Biology* 62, 423–451.
- Hopman, J., Allegranzi, B., Mehtar, S., 2020. Managing COVID-19 in low- and middle-income countries. *Jama* 323, 1549–1550.
- Hufnagel, L., Brockmann, D., Geisel, T., 2004. Forecast and control of epidemics in a globalized world. *Proceedings of the National Academy of Sciences* 101, 15124–15129.
- Kaplan, E.H., 1995. Economic analysis of needle exchange. *AIDS* 9, 1113–1120.
- Keeling, M.J., Rohani, P., 2011. *Modeling infectious diseases in humans and animals*. Princeton university press.
- Legrand, J., Grais, R.F., Boelle, P.Y., Valleron, A.J., Flahault, A., 2007. Understanding the dynamics of Ebola epidemics. *Epidemiology & Infection* 135, 610–621.
- Lima, V.D., Johnston, K., Hogg, R.S., Levy, A.R., Harrigan, P.R., Anema, A., Montaner, J.S., 2008. Expanded access to highly active antiretroviral therapy: a potentially powerful strategy to curb the growth of the hiv epidemic. *The Journal of infectious diseases* 198, 59–67.
- Mahase, E., 2020. China coronavirus: WHO declares international emergency as death toll exceeds 200. *BMJ: British Medical Journal (Online)* 368.
- Martcheva, M., 2015. *An introduction to mathematical epidemiology*. volume 61. Springer.
- Medlock, J., Galvani, A.P., 2009. Optimizing influenza vaccine distribution. *Science* 325, 1705–1708.
- Mosadeghrad, A.M., 2014. Factors influencing healthcare service quality. *International Journal of Health Policy and Management* 3, 77.
- Ngonghala, C.N., Iboi, E., Eikenberry, S., Scotch, M., MacIntyre, C.R., Bonds, M.H., Gumel, A.B., 2020. Mathematical assessment of the impact of non-pharmaceutical interventions on curtailing the 2019 novel coronavirus. *Mathematical biosciences* 325, 108364.

- Oshitani, H., Kamigaki, T., Suzuki, A., 2008. Major issues and challenges of influenza pandemic preparedness in developing countries. *Emerging Infectious Diseases* 14, 875.
- Peak, C.M., Childs, L.M., Grad, Y.H., Buckee, C.O., 2017. Comparing nonpharmaceutical interventions for containing emerging epidemics. *Proceedings of the National Academy of Sciences* 114, 4023–4028.
- Sacchetto, D., Raviolo, M., Beltrando, C., Tommasoni, N., 2020. COVID-19 surge capacity solutions: Our experience of converting a concert hall into a temporary hospital for mild and moderate COVID-19 patients. *Disaster Medicine and Public Health Preparedness* , 1–4.
- Senapati, A., Sardar, T., Ganguly, K.S., Ganguly, K.S., Chattopadhyay, A.K., Chattopadhyay, J., 2019. Impact of adult mosquito control on dengue prevalence in a multi-patch setting: a case study in Kolkata (2014–2015). *Journal of Theoretical Biology* 478, 139–152.
- Siegel, J.D., Rhinehart, E., Jackson, M., Chiarello, L., 2007. 2007 guideline for isolation precautions: preventing transmission of infectious agents in health care settings. *American journal of infection control* 35, S65–S164.
- WHO, 2005. Who checklist for influenza pandemic preparedness planning.
- WHO, 2020. Coronavirus disease 2019 (COVID-19): situation report, 73.
- Worby, C.J., Chang, H.H., 2020. Face mask use in the general population and optimal resource allocation during the COVID-19 pandemic. *Nature communications* 11, 1–9.
- Zaric, G.S., Barnett, P.G., Brandeau, M.L., 2000a. Hiv transmission and the cost-effectiveness of methadone maintenance. *American journal of public health* 90, 1100.
- Zaric, G.S., Brandeau, M.L., 2001. Optimal investment in a portfolio of hiv prevention programs. *Medical Decision Making* 21, 391–408.
- Zaric, G.S., Brandeau, M.L., Barnett, P.G., 2000b. Methadone maintenance and hiv prevention: a cost-effectiveness analysis. *Management Science* 46, 1013–1031.

Zhang, J., Litvinova, M., Liang, Y., Wang, Y., Wang, W., Zhao, S., Wu, Q., Merler, S., Viboud, C., Vespignani, A., et al., 2020a. Changes in contact patterns shape the dynamics of the COVID-19 outbreak in China. *Science* 368, 1481–1486.

Zhang, R., Li, Y., Zhang, A.L., Wang, Y., Molina, M.J., 2020b. Identifying airborne transmission as the dominant route for the spread of covid-19. *Proceedings of the National Academy of Sciences* 117, 14857–14863.